



Supported in Part By  
U.S. DEPARTMENT OF  
**ENERGY**

Office of Science

# Measurements of Vector Mesons in Ultra-Peripheral Collisions at STAR

Xihe Han

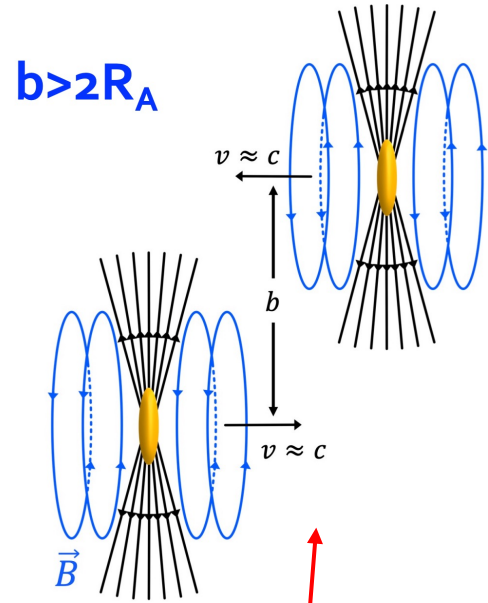
The Ohio State University

2026 RHIC/AGS User's Meeting

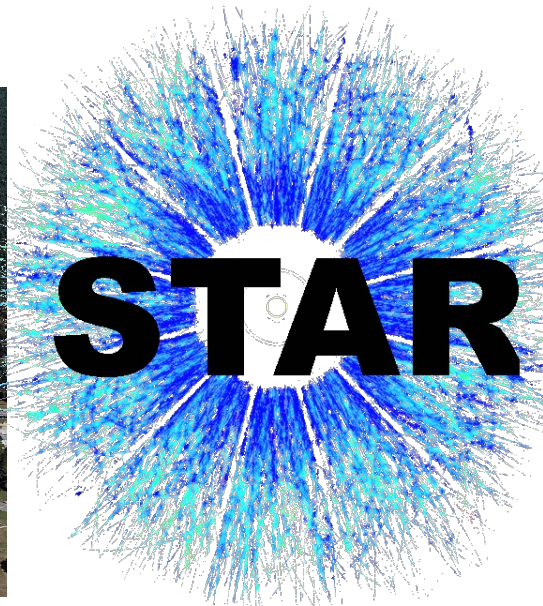
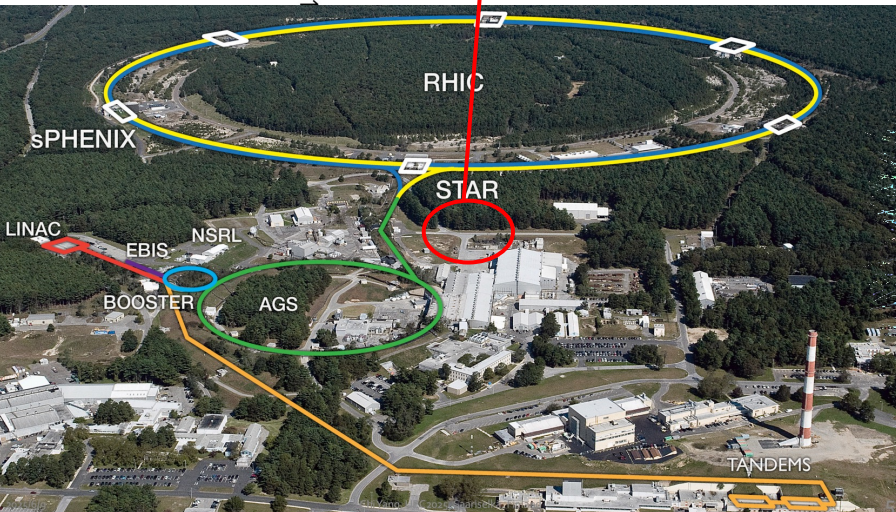


Sincerely apologize in advance for any omissions or misinterpretations ☹️

# Basics on Ultra-Peripheral Collisions (UPCs)



- **No hadronic overlap**
- **Long-range electromagnetic interactions dominate.**



RHIC/AGS

**No hadronic overlap  $\neq$  no physics.**

# Heavy Ions as Sources of (Quasi) Real Photons

- V. Weizsacker, E.J. Williams- Equivalent Photon Approximation

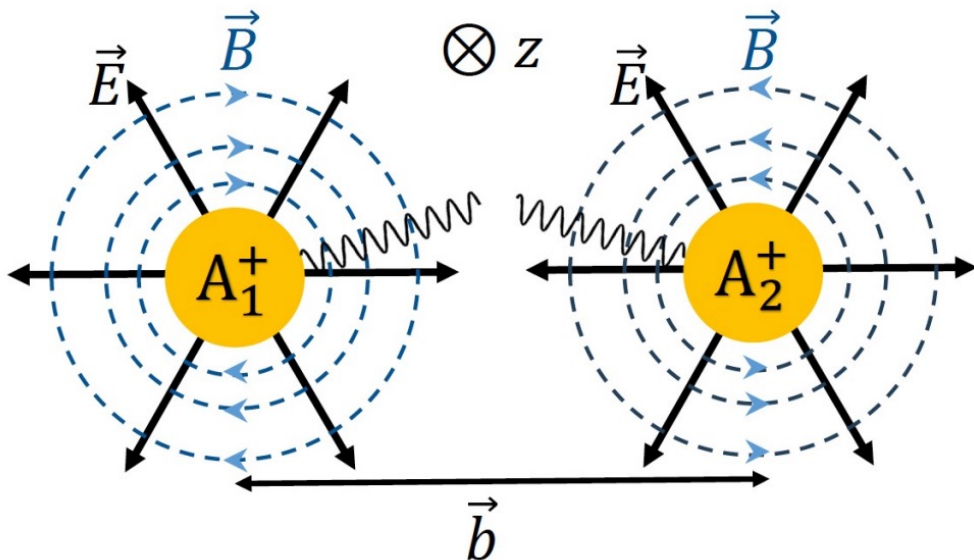
$$N(k, b) = \frac{Z^2 \alpha}{\pi^2} \frac{k}{(\hbar c)^2} \frac{1}{\gamma^2} [K_1^2(x) + \frac{1}{\gamma^2} K_0^2(x)]$$

A highly Lorentz-boosted EM Field: Flux of **quasi-real** photons

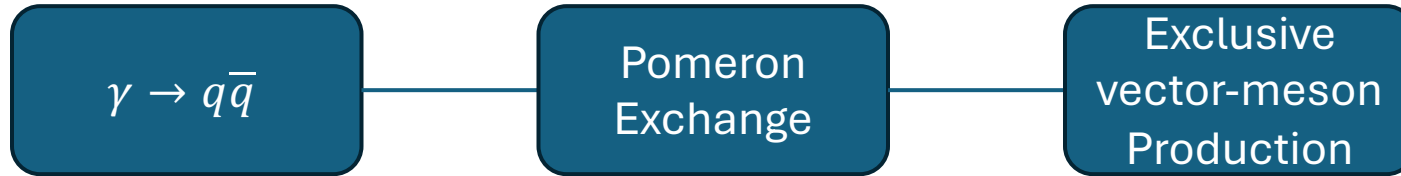
$$\text{Virtuality } Q^2 \sim \left(\frac{\hbar}{R_A}\right)^2 \sim 30 \text{ MeV}^2$$

Mostly transversely polarized

$$\omega_{\text{max}} \sim \frac{\gamma \hbar c}{R_A} \sim 3.0 \text{ GeV} \rightarrow \text{an excellent source of quasi-real photons.}$$



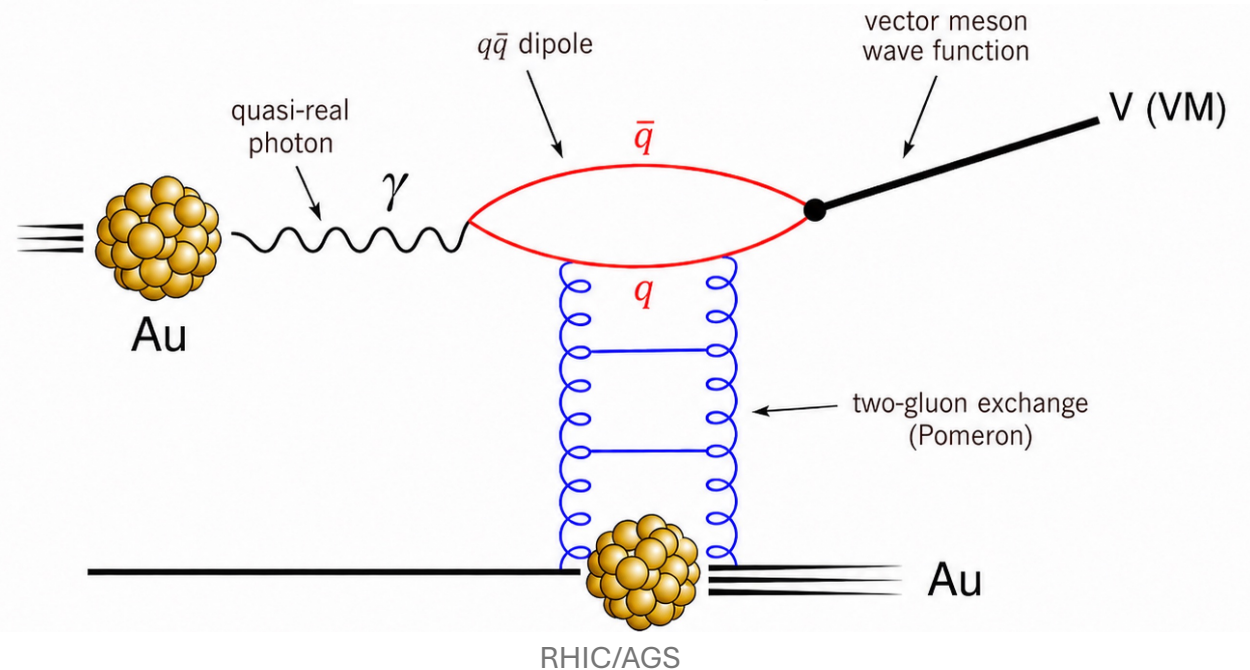
# How photons interact via the strong force



$$\sigma_{\gamma^*+A \rightarrow V+A}$$

$$\sigma_{AA \rightarrow VA} \sim \text{Photon Flux} \cdot \sigma_{\gamma A \rightarrow VA}$$

$$= \int d^2 b_{\perp} \left| \int \frac{d^2 x_{\perp}}{4\pi} \int_0^1 \frac{dz}{z(1-z)} \Psi^{\gamma^* \rightarrow q\bar{q}}(\vec{x}_{\perp}, z) N(\vec{x}_{\perp}, \vec{b}_{\perp}, Y) \Psi^V(\vec{x}_{\perp}, z)^* \right|^2$$

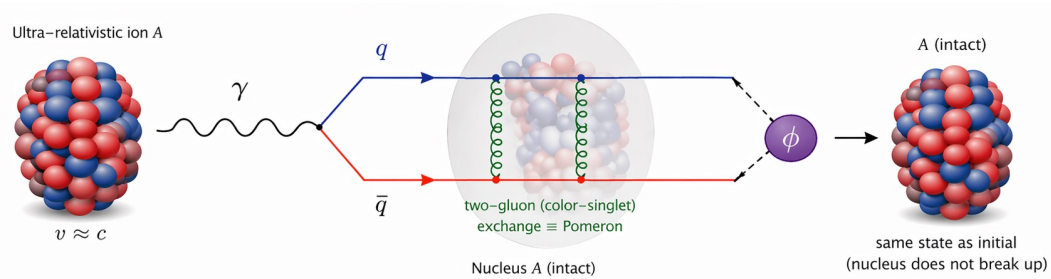


# Exclusive Vector Meson Production in UPCs

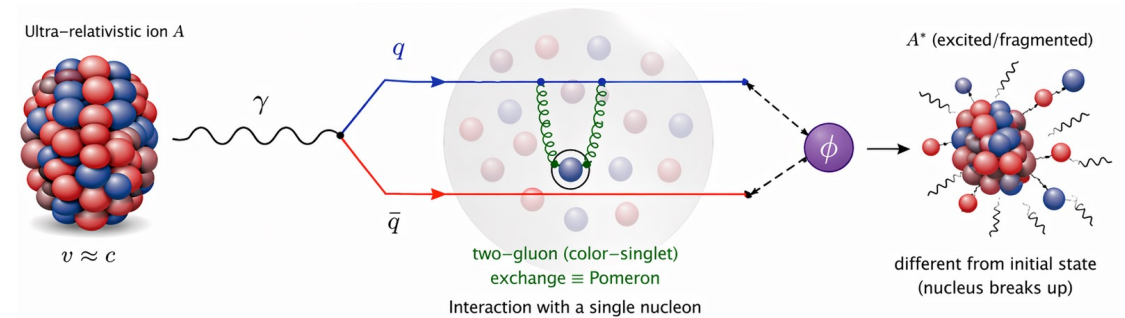
- $\gamma A \rightarrow VA$  process:

1. A quasi-real photon from the Lorentz-contracted EM field fluctuates into a  $q\bar{q}$  pair.
2. This neutral color dipole interacts with the nucleus via a colorless 2-gluon exchange (Pomeron).
3. The exclusive interaction produces a vector meson:  $\rho^0, \phi, J/\psi \dots$
4. We detect the decay products of the vector meson.

## Coherent Production



## Incoherent Production



- Interaction with the entire nucleus
- Target stays intact

- Small momentum transfer
- Sharp peak at  $|t| \approx \left| \frac{\hbar}{R_A} \right|^2$

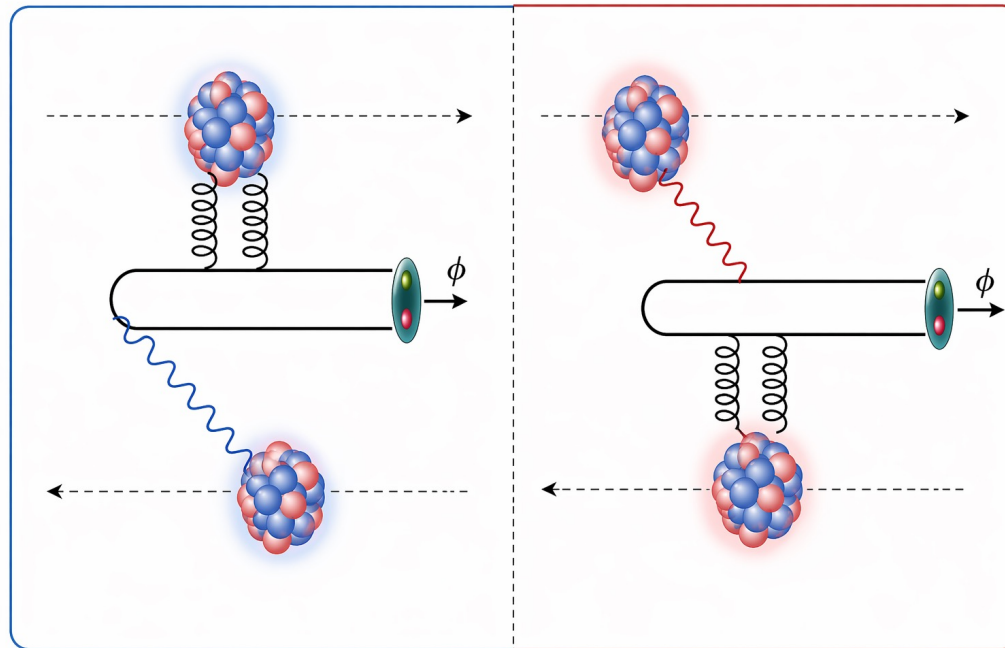
- Only one or a few nucleons participate
- Target is excited or breaks up

- Large momentum transfer
- Broad distribution in  $|t|$

# Emission ambiguity in UPCs

- When identical beams collide, there is an ambiguity about which nucleus emitted the photon, leading to **quantum interference**.
- The ambiguity exists for both coherent and incoherent processes.

Low energy photon  
High energy target  
 $k = \frac{M_V}{2} e^{-y}, x = \frac{M_V}{\sqrt{s}} e^{+y}$

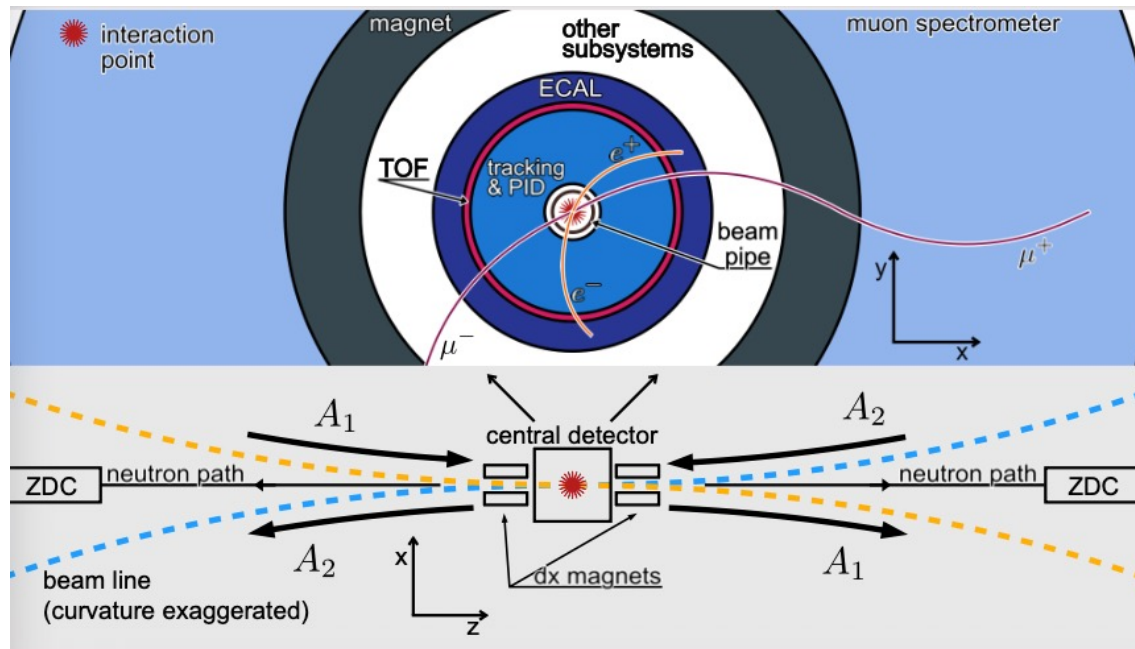


High energy photon  
Low energy target  
 $k = \frac{M_V}{2} e^{+y}, x = \frac{M_V}{\sqrt{s}} e^{-y}$

$$\frac{d\sigma_{AA \rightarrow AAV}}{dy} = k \frac{dN}{dk}(k_1) \sigma_{\gamma A \rightarrow VA}(k_1) + k \frac{dN}{dk}(k_2) \sigma_{\gamma A \rightarrow VA}(k_2)$$

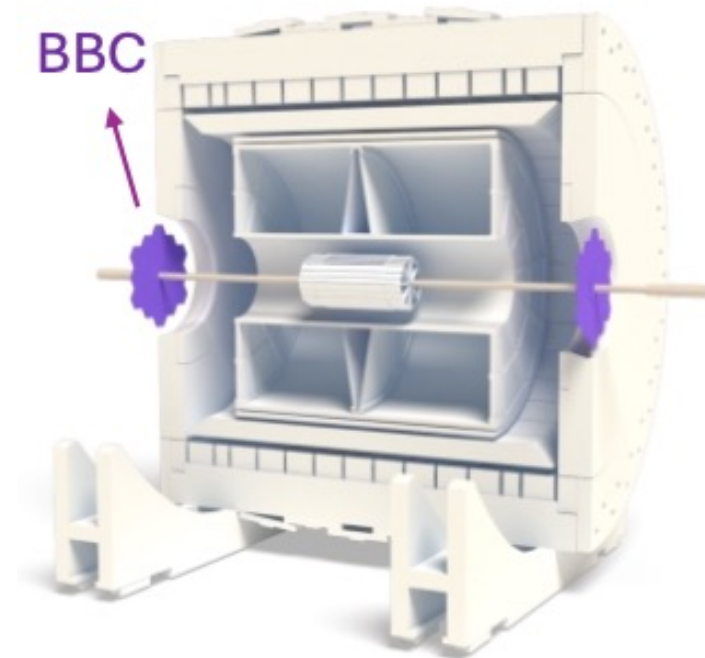
# The STAR Detector and UPCs

UPC exclusive production signatures:  
**Minimal hadronic activity**  
**Forward rapidity gap**



*Cross-sectional and longitudinal view of the STAR detector*

ZDC (Zero Degree Calorimeter): Detects forward neutrons from **Coulomb dissociation**, allowing classification of nuclear breakup and triggering on UPC events.



*Longitudinal view highlighting BBC*

BBC (Beam-Beam Counter): helps veto hadronic interactions by **requiring no forward charged activity**.

# Early Measurements

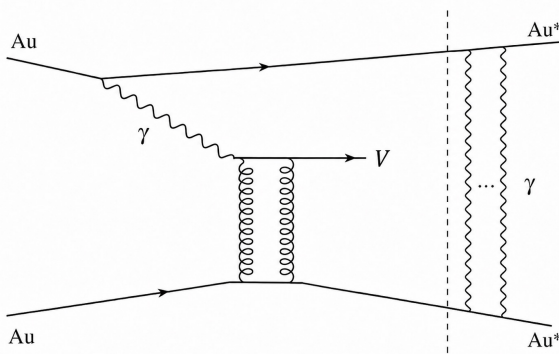
# Early Measurement – Coherent $\rho^0$ Photoproduction

STAR, *Phys. Rev. Lett.* **89** (2002) 272302.

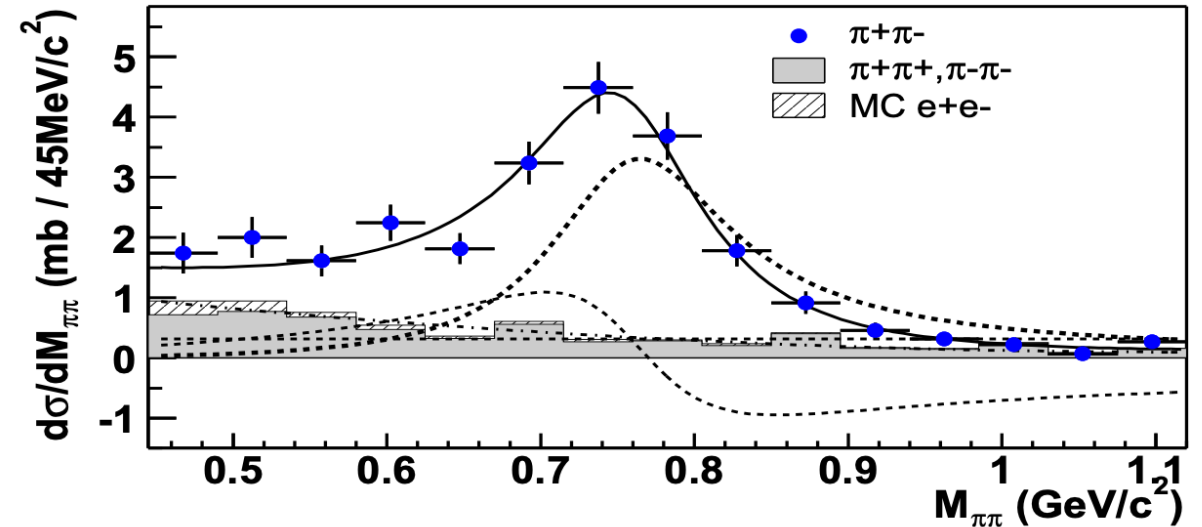
- Year 2000
- Au+Au at  $\sqrt{s_{NN}} = 130\text{GeV}$
- Half Field
- “topological Trigger” + ZDCMB (59 inv mb)

## Foundational STAR UPC vector meson paper

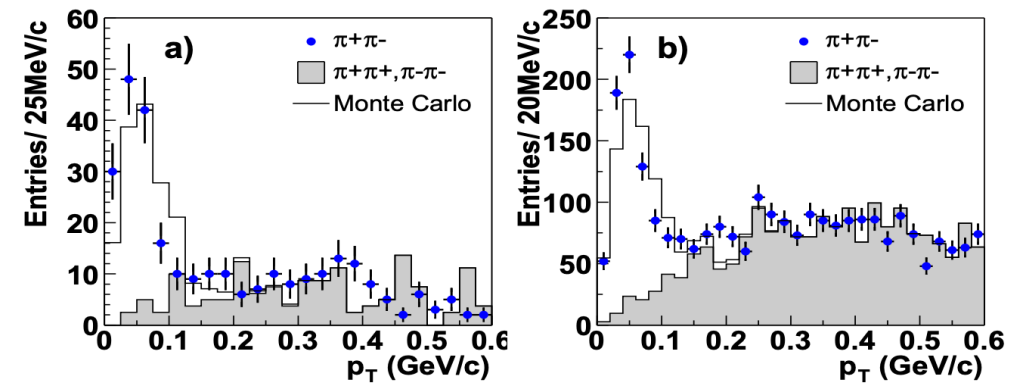
Established UPC events can be studied by triggering on **mutual Coulomb excitation**.



Separated measurements into **different neutron emission classes (0n0n, 0nXn, XnXn...)**



First UPC  $\frac{d\sigma_{\rho^0}}{dM_{\pi\pi}}$  measurement with pair  $p_T < 150\text{ MeV}/c$  in ZDCMB data at STAR



$p_T$  spectra demonstrating coherent peak by (a) topological trigger and (b) ZDCMB

# Two-source Interference in UPC Photoproduction

STAR, *Phys. Rev. Lett.* **102** (2009) 112301.

Au+Au at  $\sqrt{s_{NN}} = 200$  GeV.

Recall: Two source ambiguity as **quantum interference**

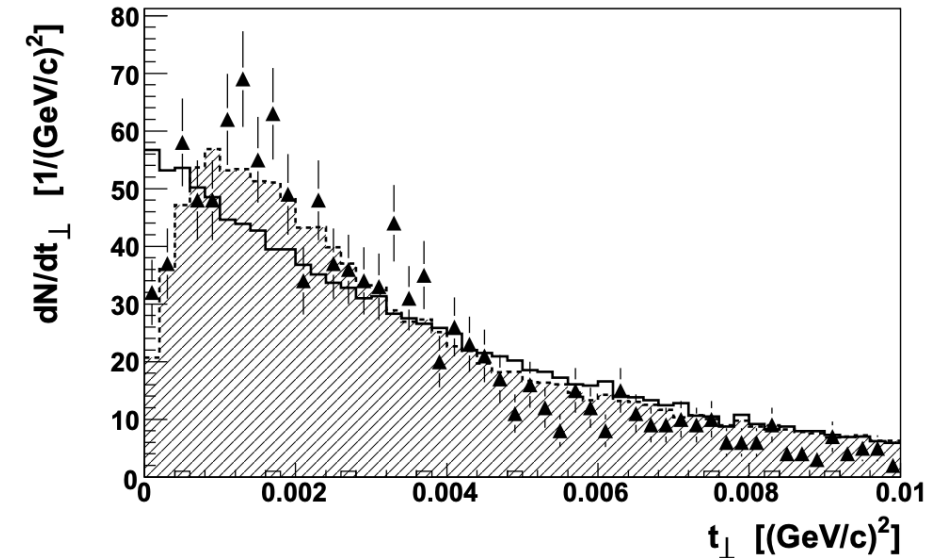
For vector mesons,  $J^{PC} = 1^{--}$

Exchanging role of two nuclei – parity transformation.

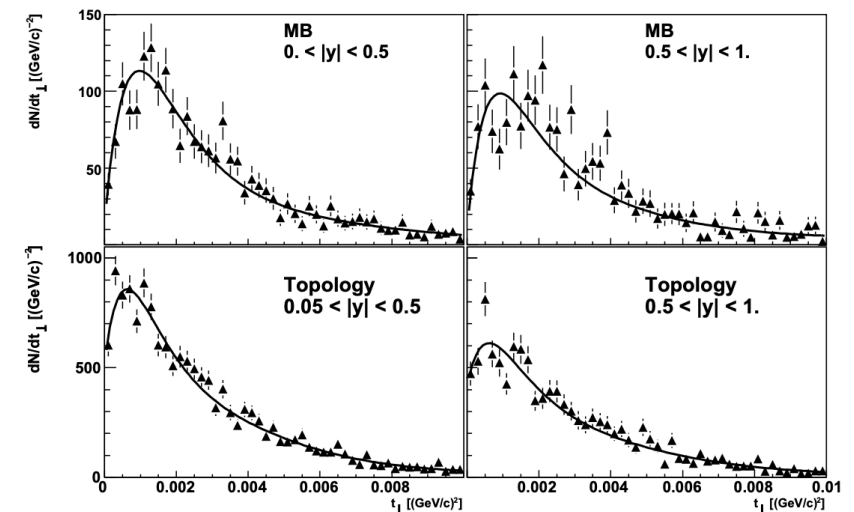
$$A_{tot} = A_1 - A_2 e^{ip_T \cdot b}$$

At midrapidity where  $|A_1| \sim |A_2|$ , and low  $|t| = p_t^2$ : **Suppression**

**From cross section to quantum interference, confirmed.**



Uncorrected  $\rho^0 t$  spectrum comparing data with simulation that includes quantum interference (dashed line) and simulation without interference (black line).



Corrected  $\rho^0 t$  spectrum in midrapidity (left) and higher rapidity (right) regions

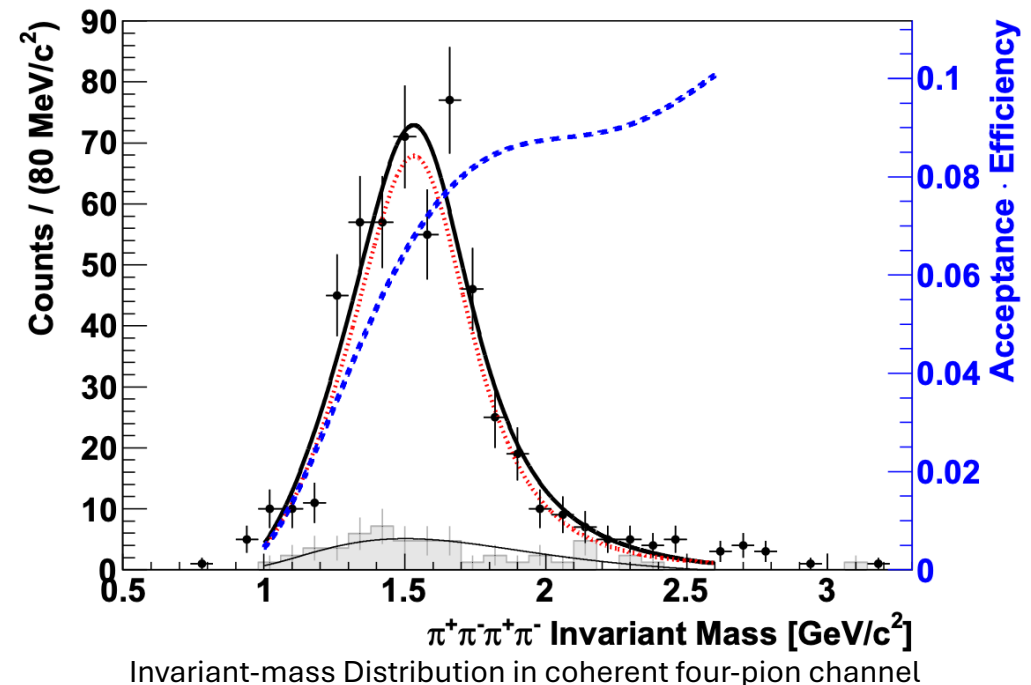
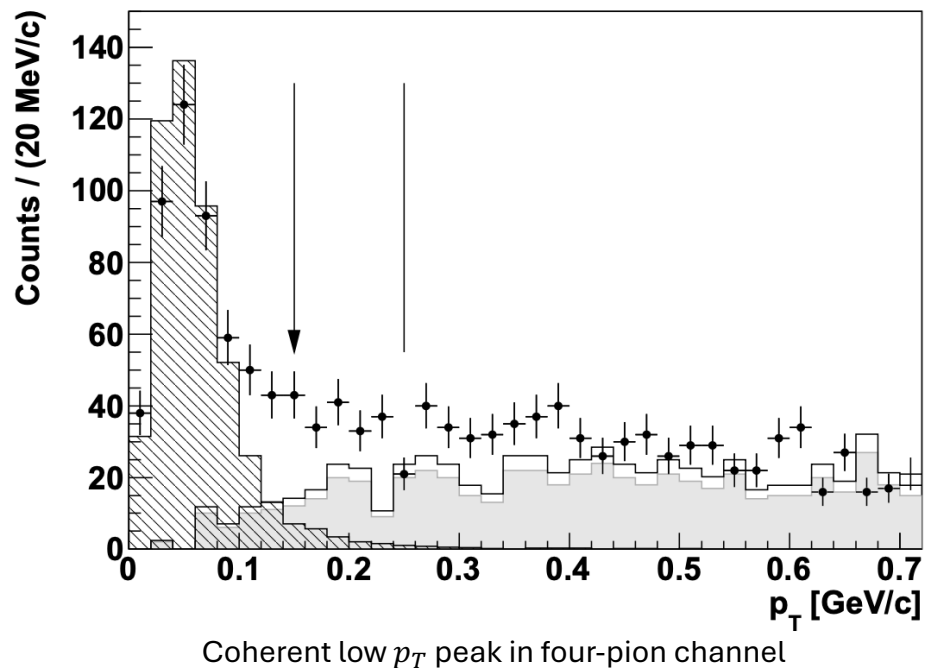
# Excited $\rho$ in UPC Photoproduction via Four-Pion

STAR, Phys. Rev. C **81** (2010) 044901.

2007, Au+Au at  $\sqrt{s_{NN}} = 200$  GeV

Extends the STAR UPC program beyond the ground-state  $\rho^0$  and into excited light-vector phenomenology through coherent four-pion photoproduction.

The PDG currently lists two excited  $\rho^0$  states, the  $\rho^0(1450)$  and the  $\rho^0(1700)$ , which are seen in various production modes and decay channels including two- and four-pion final states [4]. The nature of these states is still an open question, because their decay patterns do not match quark model predictions [5]. Little data exist on



# More $\rho^0$ UPC Photoproduction Measurements

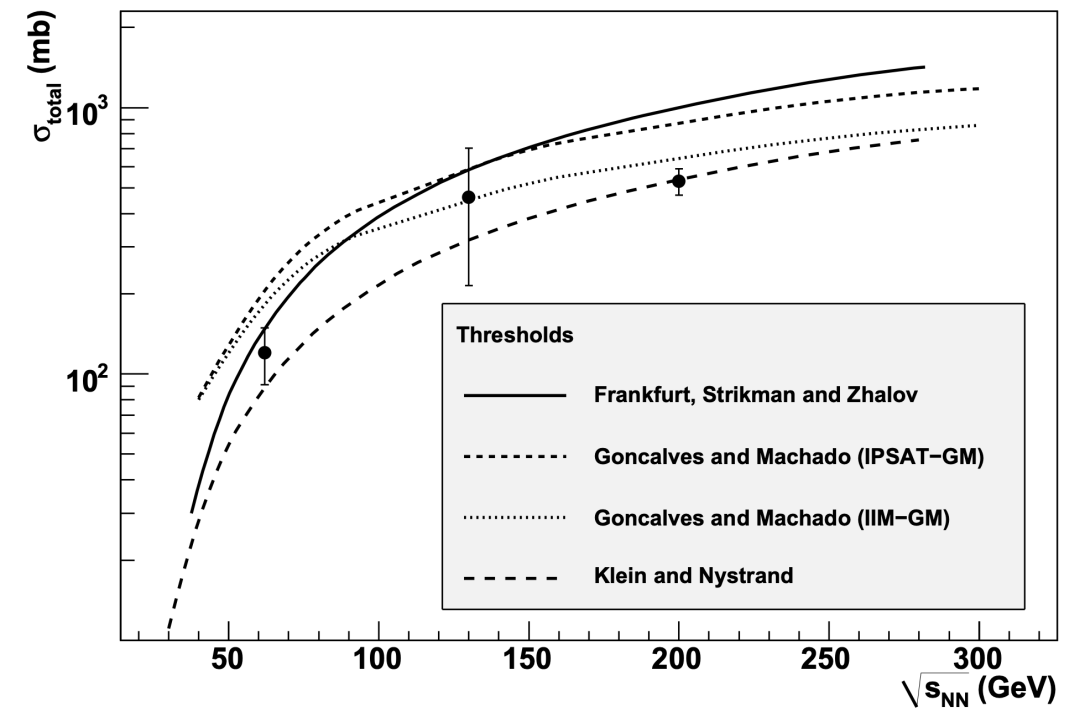
STAR, *Phys. Rev. C* **85** (2012) 014910. Au+Au at  $\sqrt{s_{NN}} = 62.4$  GeV

Parameter	STAR at $\sqrt{s_{NN}} = 62.4$ GeV coherent ( $ y_{\rho^0}  < 1$ )	STAR at $\sqrt{s_{NN}} = 62.4$ GeV coherent (full rapidity)	STAR at $\sqrt{s_{NN}} = 130$ GeV [11] coherent (full rapidity)	STAR at $\sqrt{s_{NN}} = 200$ GeV [10] coherent (full rapidity)
$\sigma_{X_n^{\rho^0} X_n}$ (mb)	$6.2 \pm 0.9 \pm 0.8$	$10.5 \pm 1.5 \pm 1.6$	$28.3 \pm 2.0 \pm 6.3$	$31.9 \pm 1.5 \pm 4.5$
$\sigma_{0n^{\rho^0} X_n}$ (mb)	$16.7 \pm 2.7 \pm 2.$	$31.8 \pm 5.2 \pm 3.9$	$95 \pm 60 \pm 25$	$105 \pm 5 \pm 15$
$\sigma_{0n0n}^{\rho^0}$ (mb)	$28.5 \pm 5.2 \pm 4.8$	$78 \pm 14 \pm 13$	$370 \pm 170 \pm 80$	$391 \pm 18 \pm 55$
$\sigma_{total}^{\rho^0}$ (mb)	$51.5 \pm 5.9 \pm 5.3$	$120 \pm 15 \pm 22$	$460 \pm 220 \pm 110$	$530 \pm 19 \pm 57$

Provides the crucial lower-energy anchor point for STAR light-meson UPC physics.

The 62.4 GeV result constrains how fast the coherent  $\rho^0$  cross section rises with collision energy.

The increase is weaker than in many theory predictions.



# The Precision Era

# 2017 $\rho^0$ Measurement

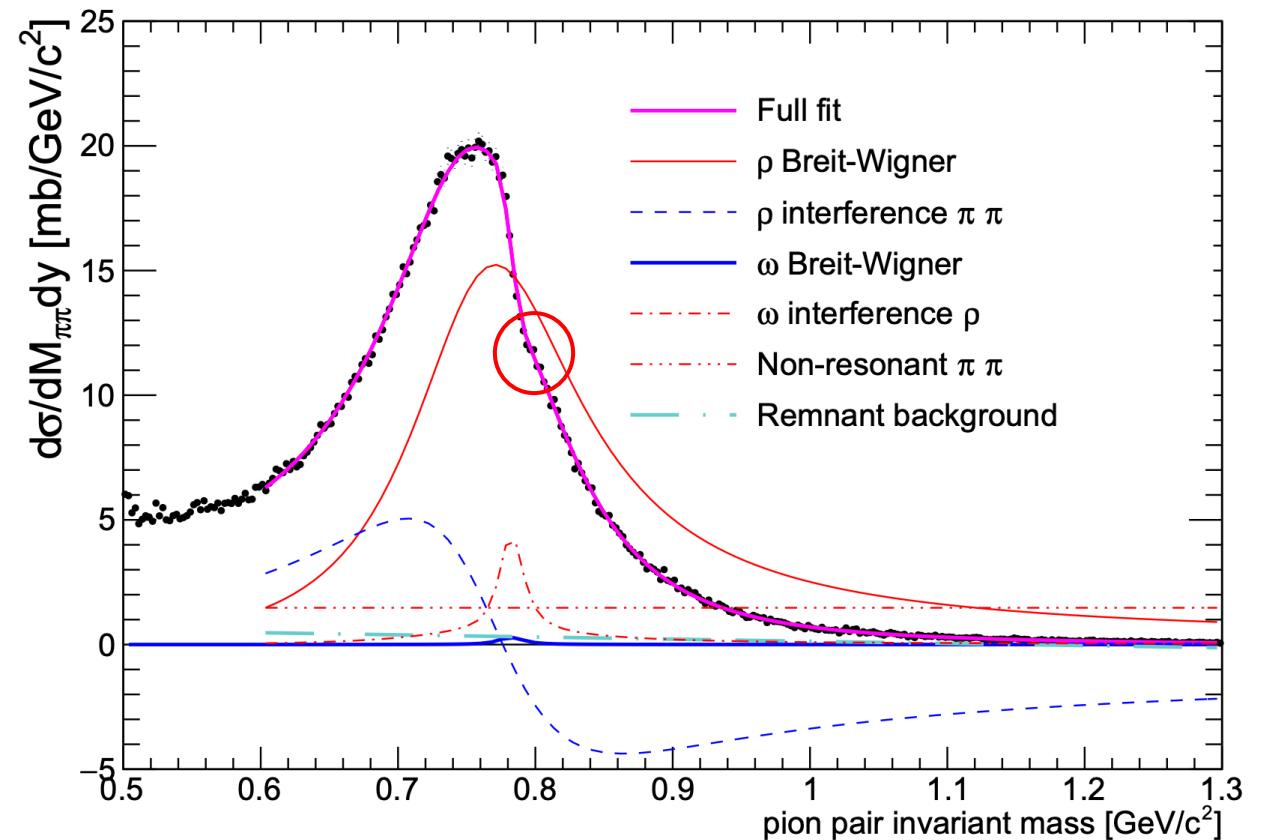
STAR, *Phys. Rev. C* **96** (2017) 054904

Run 10,  $1100 \mu b^{-1}$ , Au+Au at  $\sqrt{s_{NN}} = 200$  GeV, **Modern UPC trigger**

$$\frac{d\sigma}{dM_{\pi^+\pi^-}} \propto \left| A_\rho \frac{\sqrt{M_{\pi\pi} M_\rho \Gamma_\rho}}{M_{\pi\pi}^2 - M_\rho^2 + i M_\rho \Gamma_\rho} + B_{\pi\pi} + C_\omega e^{i\phi_\omega} \frac{\sqrt{M_{\pi\pi} M_\omega \Gamma_{\omega \rightarrow \pi\pi}}}{M_{\pi\pi}^2 - M_\omega^2 + i M_\omega \Gamma_\omega} \right|^2 + f_p$$

**First observation/extraction of the  $\omega$  meson in UPCs.**

**Simultaneous fit of  $\rho^0$ ,  $\omega$ , and nonresonant/direct  $\pi^+\pi^-$  production.**

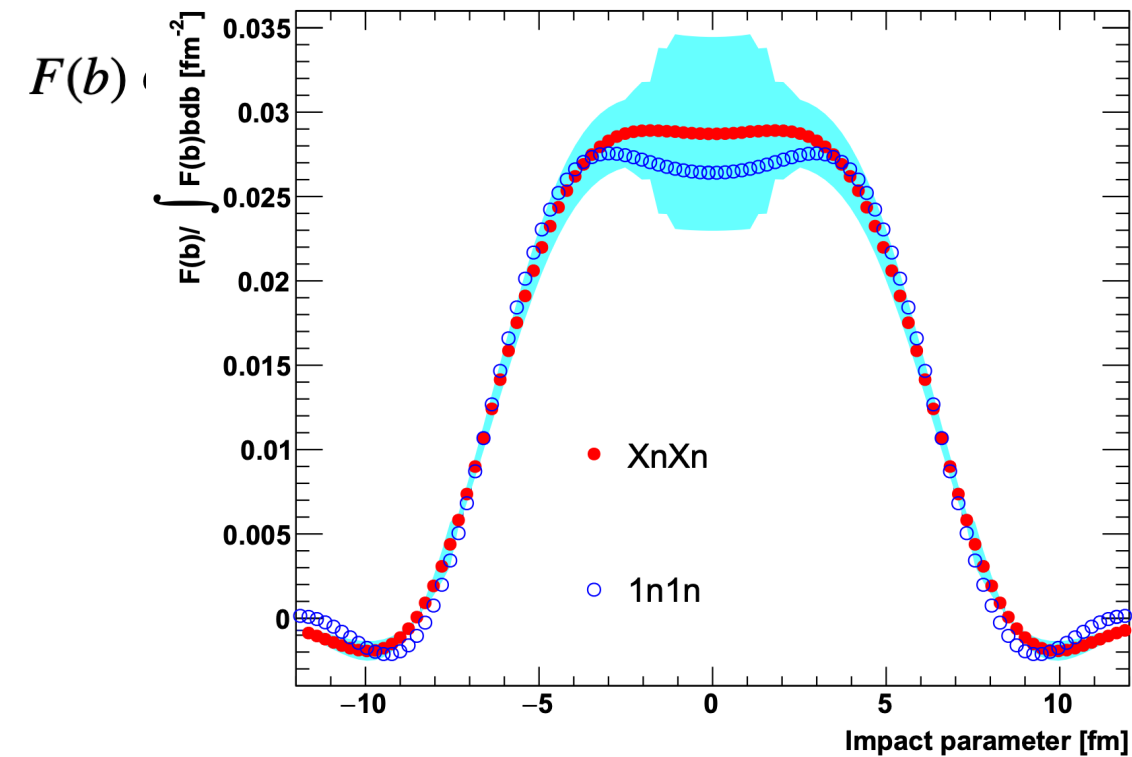


# 2017 $\rho^0$ Measurement - Tomography

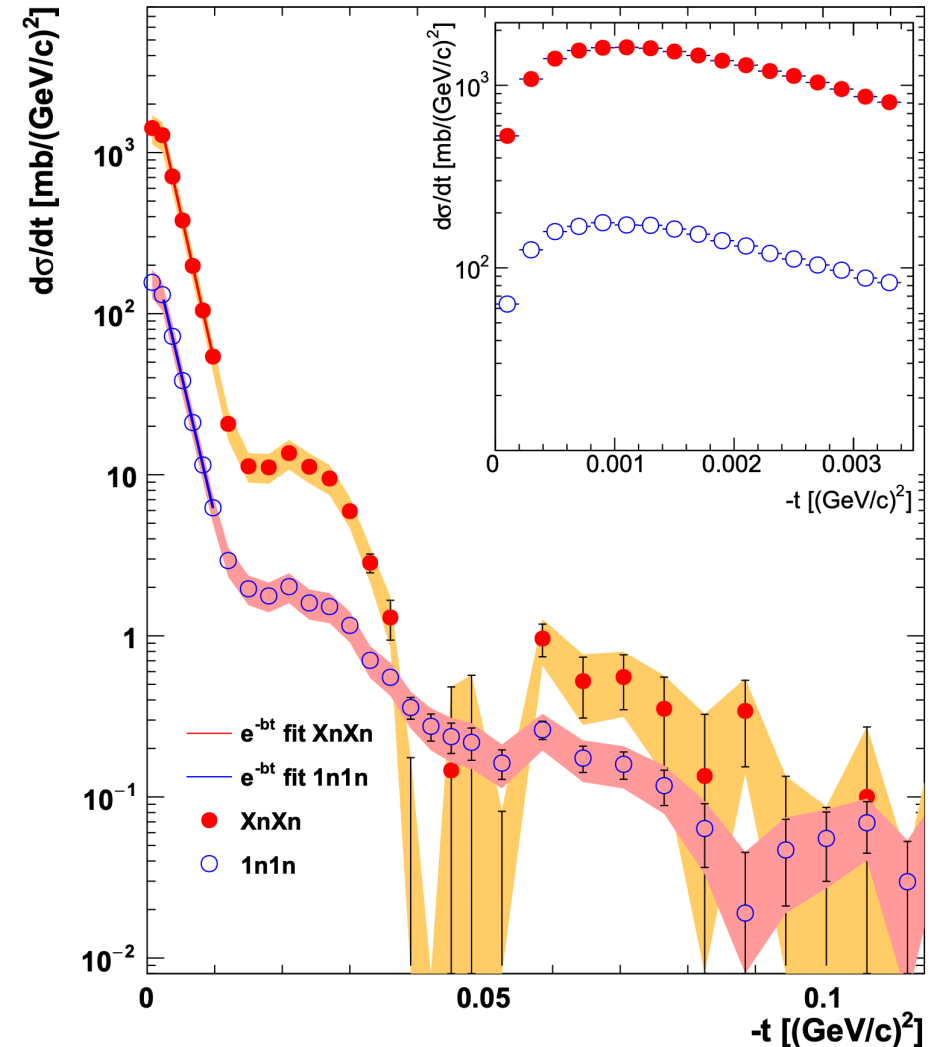
STAR, *Phys. Rev. C* **96** (2017) 054904

Run 10,  $1100 \mu b^{-1}$ , Au+Au at  $\sqrt{s_{NN}} = 200$  GeV, Modern UPC trigger

**Demonstrated coherent diffractive peaks with two minima**  
**The positions of the diffractive minima encode information about the transverse nuclear profile.**



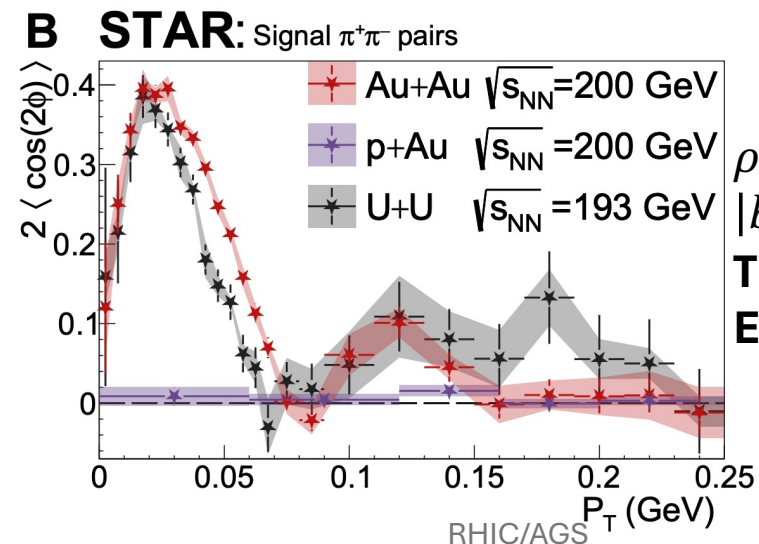
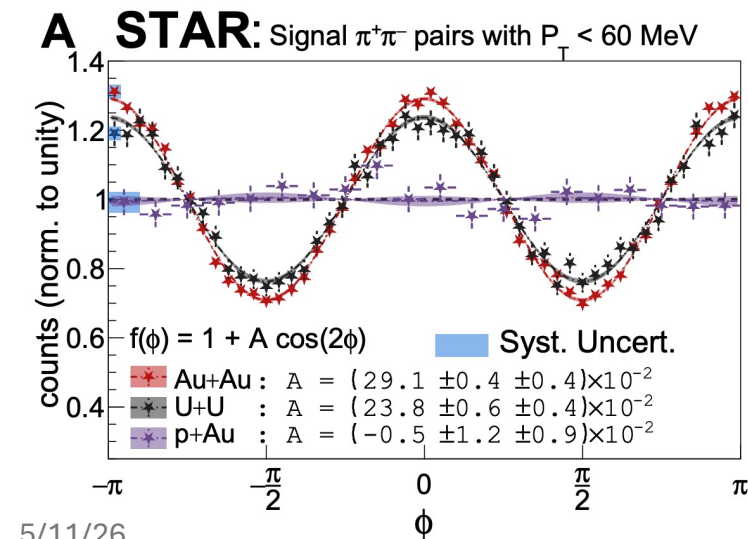
**Shows coherent diffraction of  $\rho^0$  off of an object as big as Au nuclei.**



# Tomography of Ultra-relativistic Nuclei with Polarized Photon-gluon Collisions

STAR, Sci. Adv. 9, abq3903 (2023)

- The initial photons are **linearly polarized in the transverse plane**.
- The decayed pion pair must therefore carry the angular information as orbital angular momentum:
  - $M_{\rho \rightarrow \pi\pi} \sim \epsilon_\rho \cdot q \rightarrow |M|^2 \sim \cos^2(\phi) \sim 1 + \cos(2\phi)$
- But the initial polarization axis is random event-by-event.
  - In the lab frame**, the modulation would average away.
- Two-way emission ambiguity gives an interference term involving  $P_T \cdot b$ , which makes  $P_T$  statistically correlated with the hidden initial polarization.  $\cos \phi = (p_{T1} + p_{T2}) \cdot (p_{T1} - p_{T2}) / (|p_{T1} + p_{T2}| \times |p_{T1} - p_{T2}|)$



$\rho^0$  decay time:  $\sim 1$  fm  
 $|b| \sim 10 - 20$  fm

**The final pion pair kept the interference pattern!**  
**Entanglement Enabled Intensity Interferometry**

# Tomography of Ultra-relativistic Nuclei with Polarized Photon-gluon Collisions

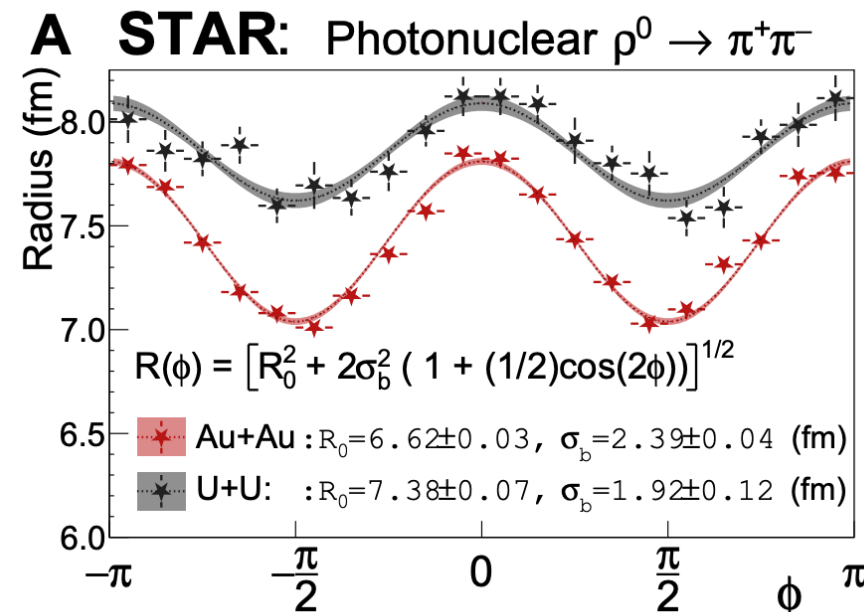
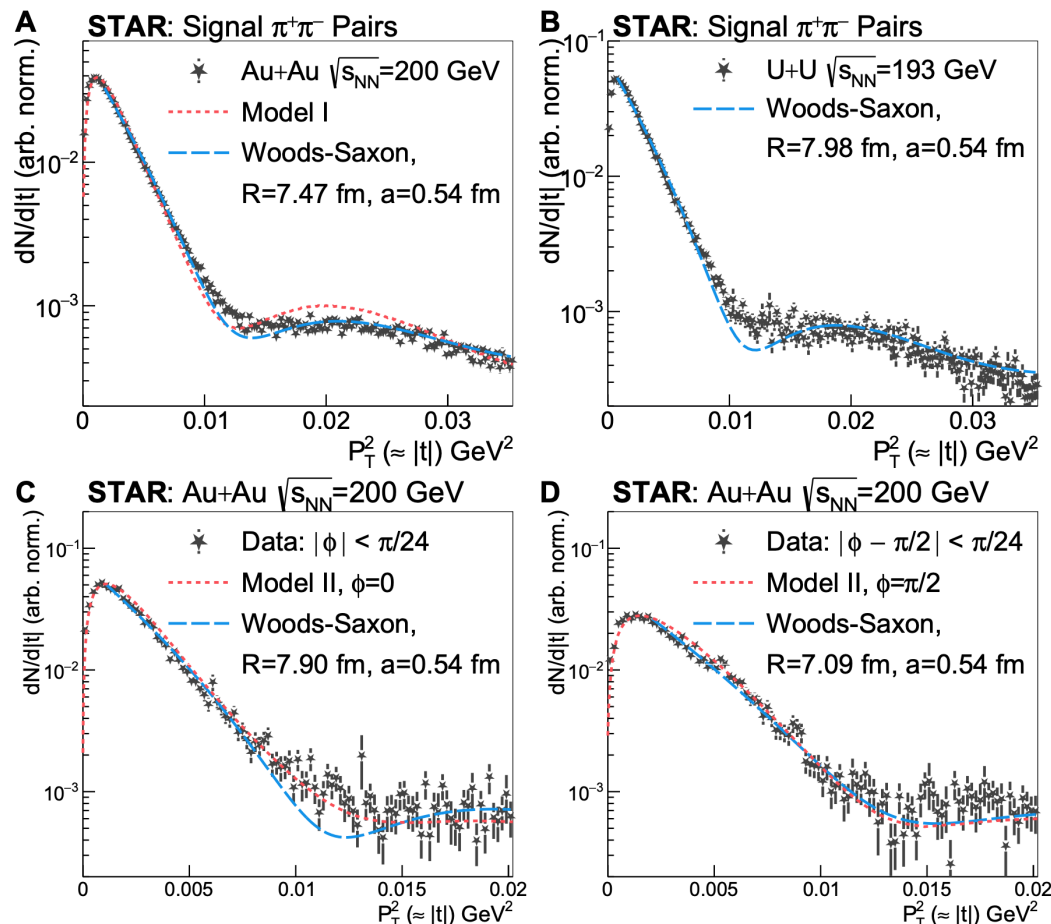
STAR, Sci. Adv. 9, abq3903 (2023)

- Recall: Tomography thorough coherent  $t$  distribution

Fit the  $|t|$  distribution with Woods Saxon FF.

$$\frac{d\sigma}{dt} \sim A|F(t)|^2, \text{ extract radius and neutron skin depth.}$$

Two source ambiguity interfere with a phase involving  $\cos(P_T \cdot b)$  alters the  $|t|$  distribution beyond very low  $|t|$  region. At  $\phi = 90^\circ$ , interference effect is minimized. One can fit  $\frac{dN}{d|t|}$  in  $\phi$  slices and account for  $\rho^0$  probe size



Result:  $R_{Au} = 6.53 \pm 0.03(\text{stat.}) \pm 0.05(\text{syst})$  fm

# Spin Interference in $J/\psi$

STAR, [arXiv:2512.02865](https://arxiv.org/abs/2512.02865). Submitted to Phys. Rev. Lett

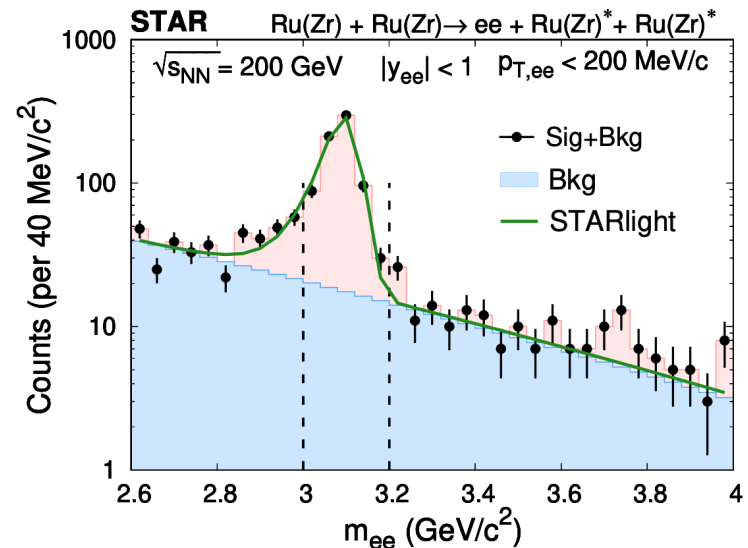
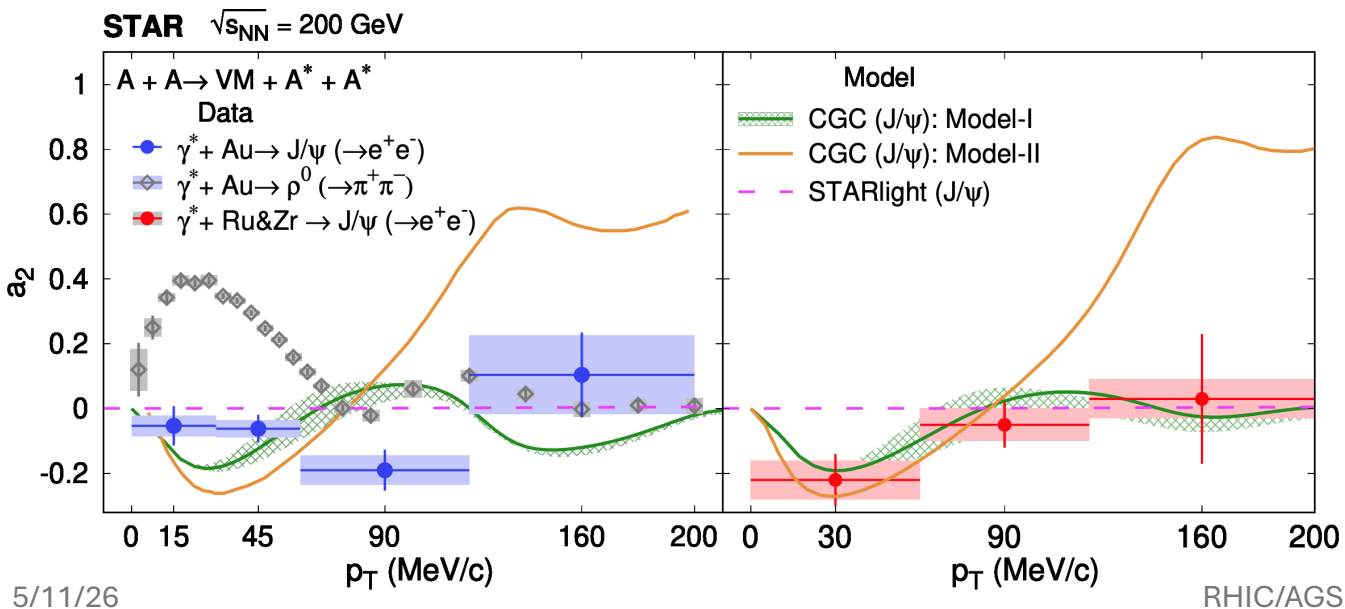
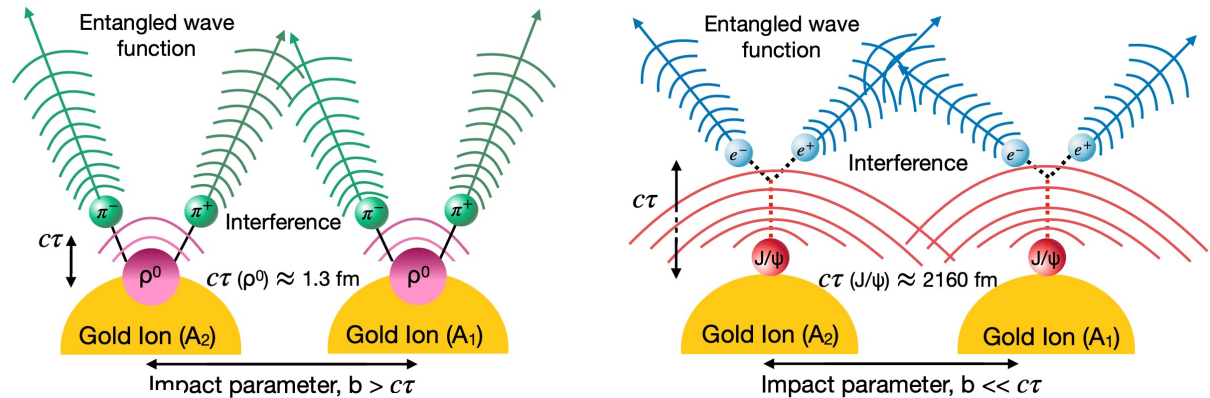
Au+Au, Ru+Ru, Zr+Zr,  $\sqrt{s_{NN}} = 200$  GeV

Evidence that the spin structure of the **final-state daughters**.

The long lifetime allows the quantum state to evolve and interfere well beyond the nuclear volume.

Compared with  $\rho^0$ ,  $J/\psi$  has:

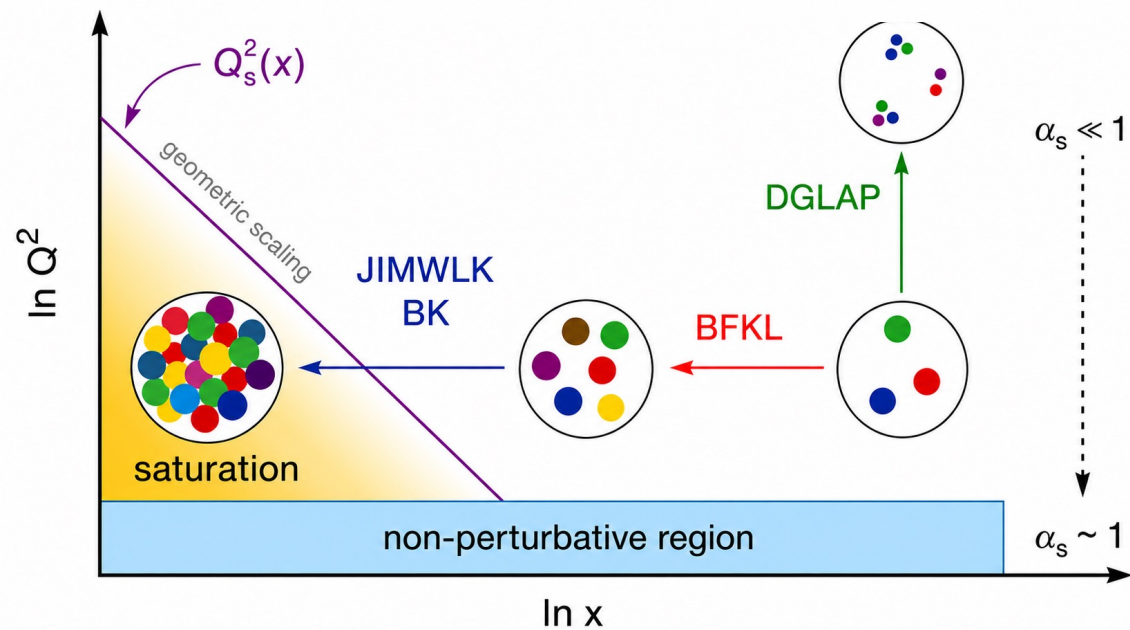
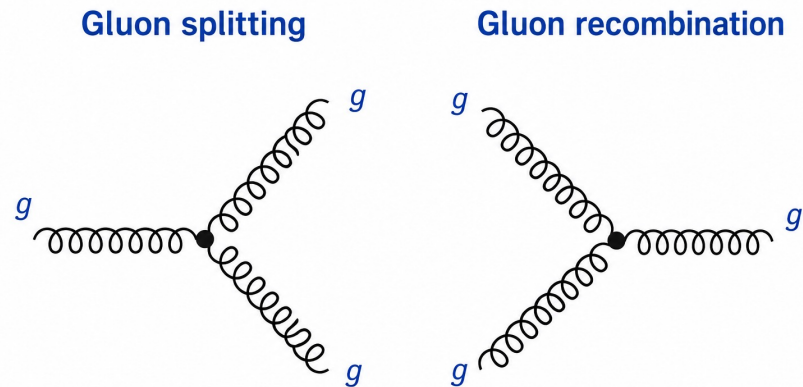
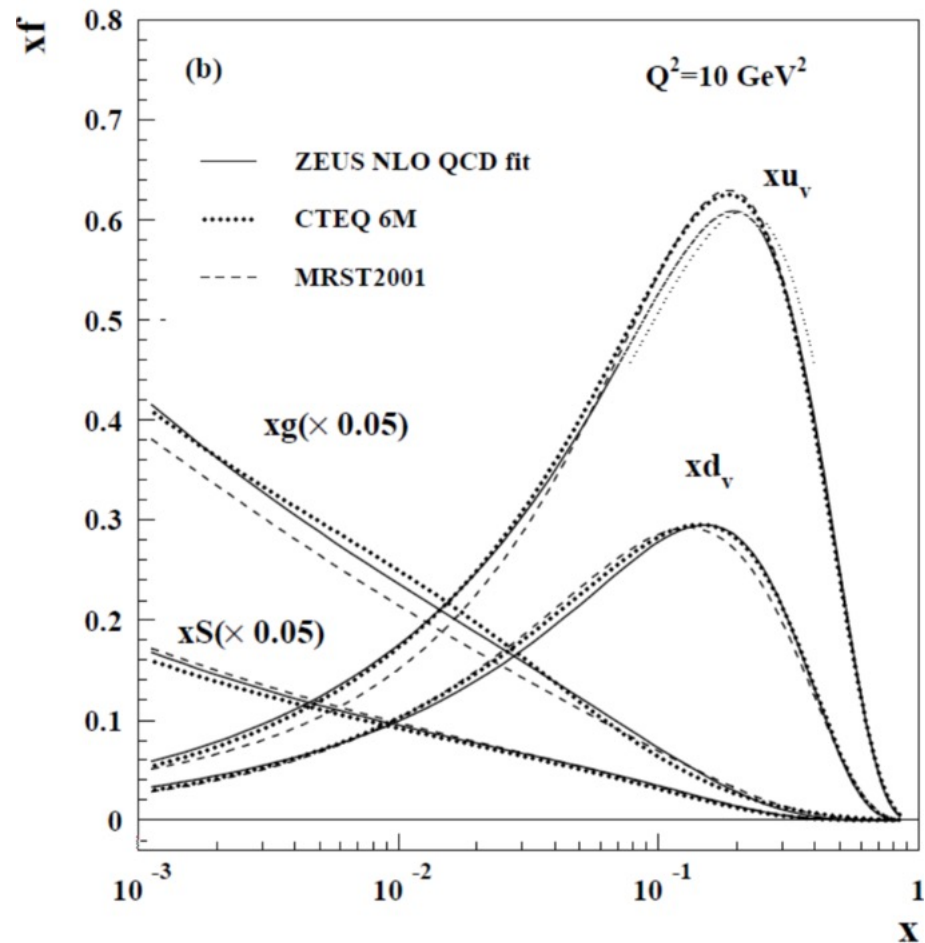
1. Longer life-time
2. **Fermion** decay products



# Connecting to EIC Physics

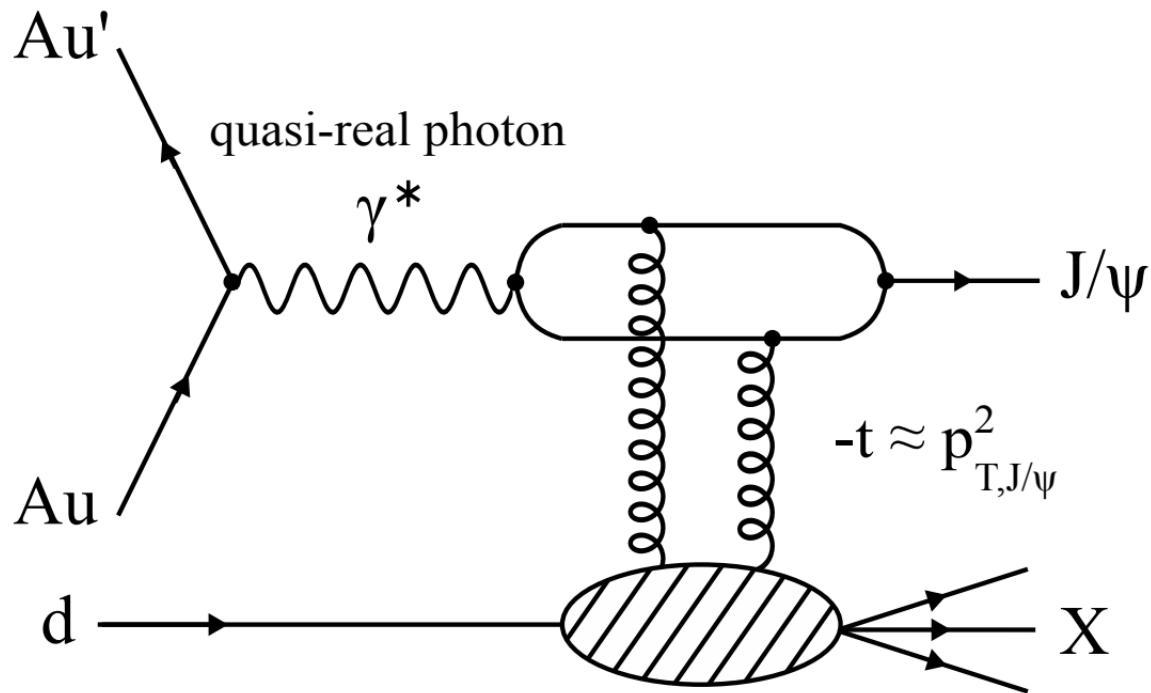
# UPCs as Probes of Gluon Structure

- Shadowing: The nucleus has fewer effective gluons than  $A$  free nucleons.
- Saturation: Gluon field becomes so dense that nonlinear recombination matters.



# Resolving the Two-Way Ambiguity

- Use an asymmetric collision system.



$$k = \frac{M_{J/\psi}}{2} e^{-y}, W_{\gamma N} = \sqrt{2\sqrt{s_{NN}} k} \sim 25 \text{ GeV}$$

Vary  $J/\psi$  rapidity  $\rightarrow$  Changing photon energy

# $J/\psi$ Production in d+Au

STAR, Phys. Rev. Lett. **128**(2022) 122303.

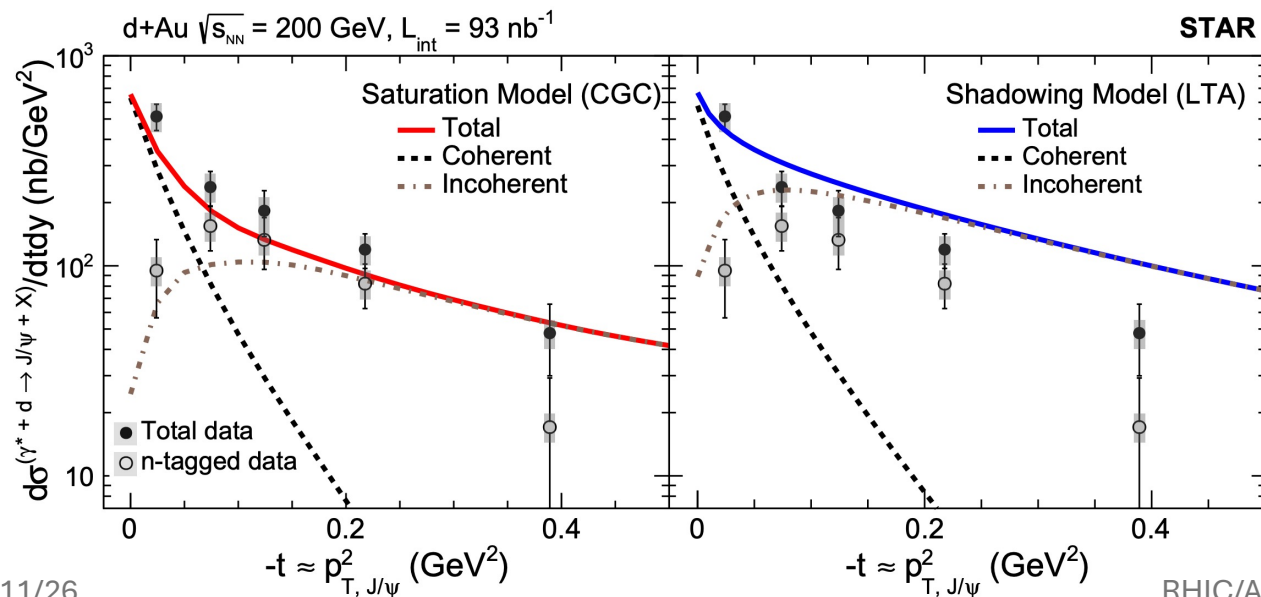
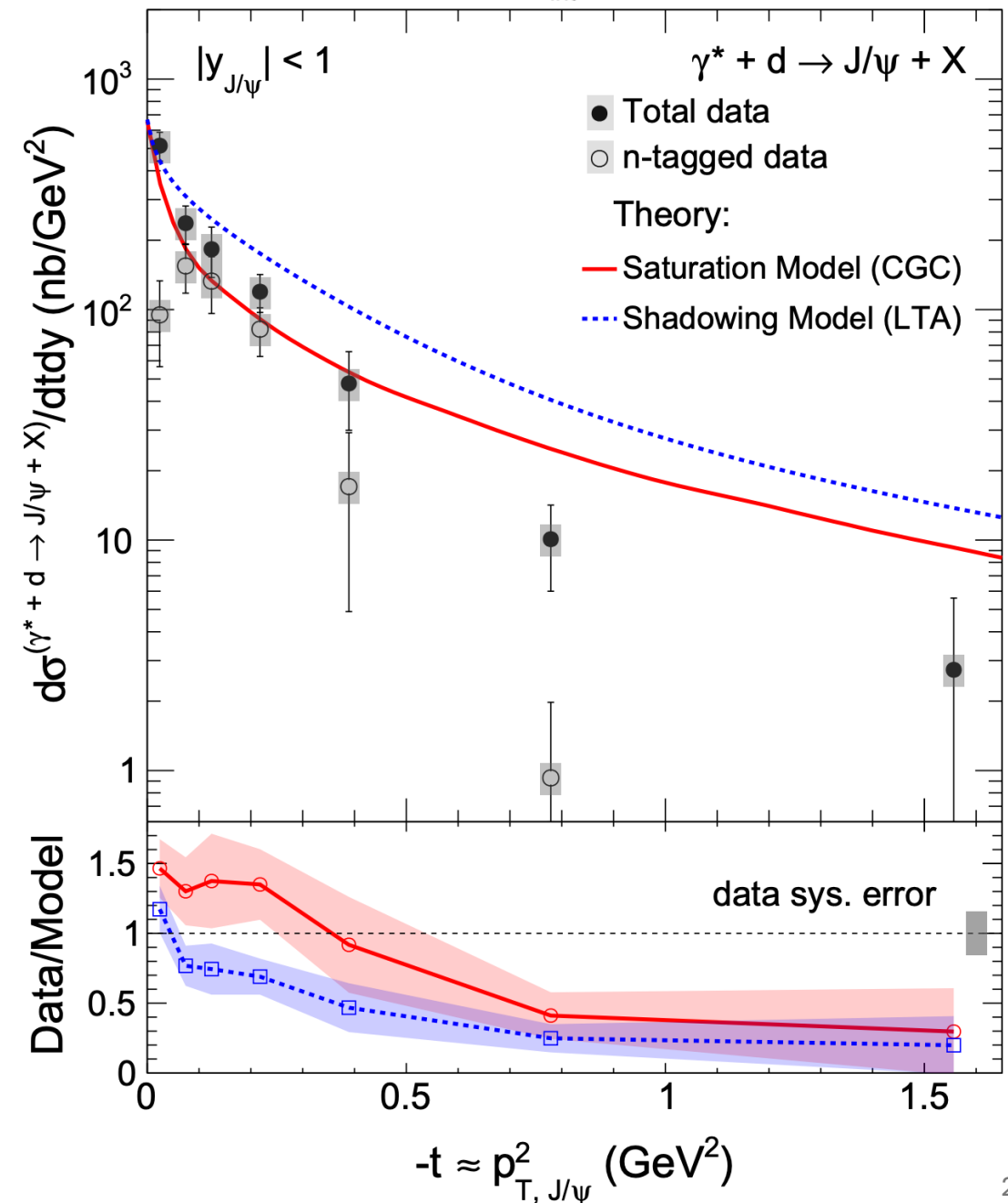
Run 16 d+Au at  $\sqrt{s} = 200$  GeV

**Neutron tagged = incoherent dominant**

Data can already discriminate among different pictures of deuteron gluon structure, with **saturation-based descriptions giving a better account of the measured distributions than the shadowing model.**

d+Au  $\sqrt{s_{NN}} = 200$  GeV,  $L_{int} = 93$  nb $^{-1}$

STAR

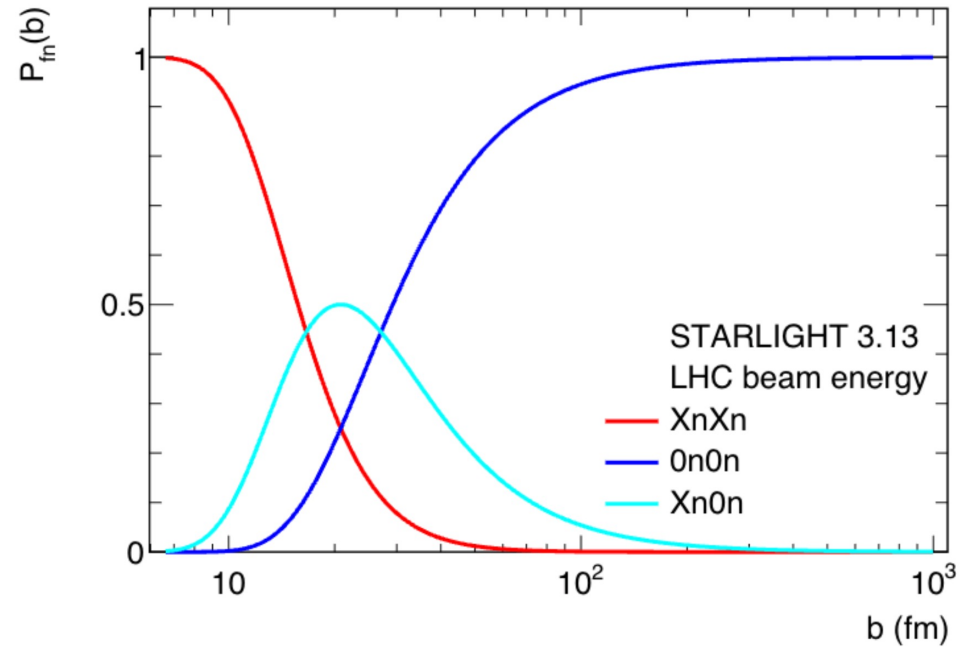
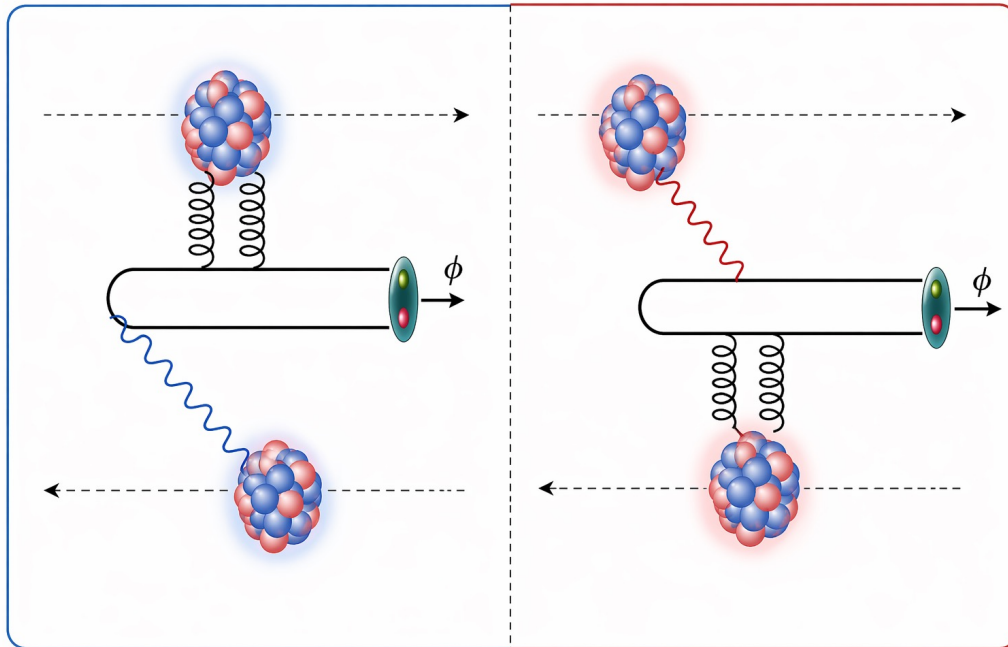


Data/Model

data sys. error

# Resolving the Two-Way Ambiguity – cont.

$$\frac{d\sigma_{AA \rightarrow AAV}}{dy} = k \frac{dN}{dk}(k_1) \sigma_{\gamma A \rightarrow VA}(k_1) + k \frac{dN}{dk}(k_2) \sigma_{\gamma A \rightarrow VA}(k_2)$$



- Photon flux factors are **impact-parameter dependent**.
  - Different impact parameter  $\rightarrow$  photon flux distribution changes, but  $\sigma_{\gamma A \rightarrow VA}$  does not.
- We can gauge the impact parameter distribution via **different neutron tagging**
  - $\frac{d\sigma}{dy}$  measurement with different neutron tagging allows us to solve for  $\sigma_{\gamma A \rightarrow VA}$

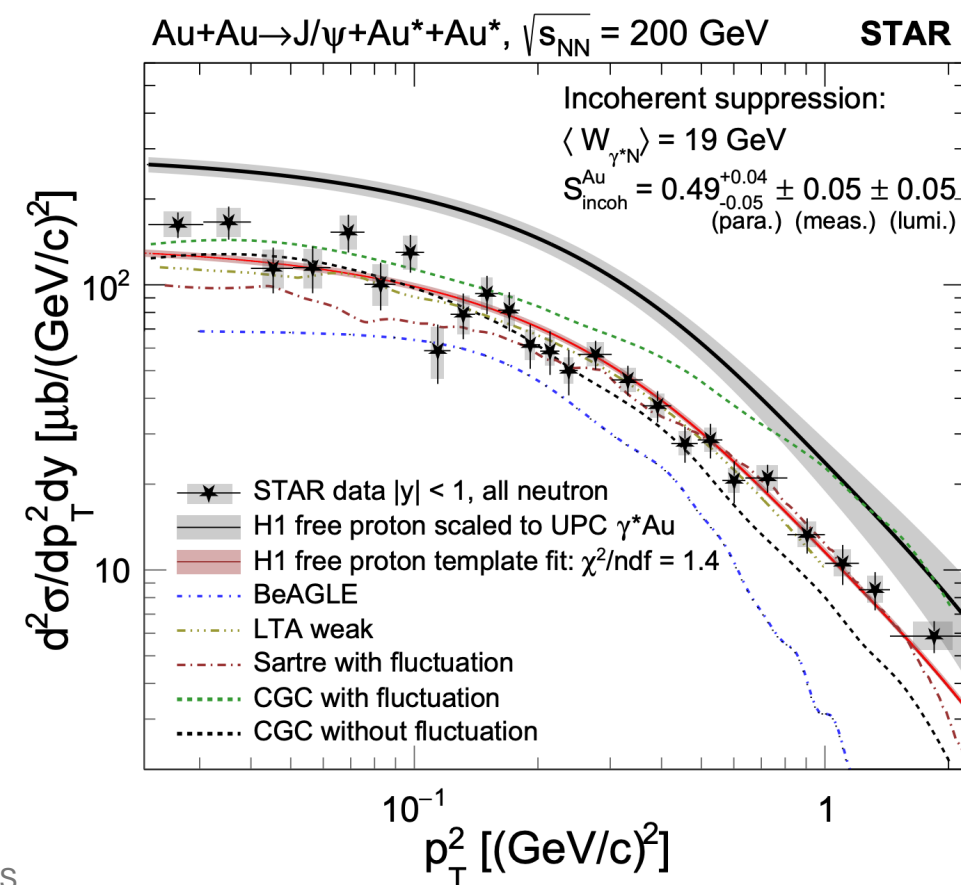
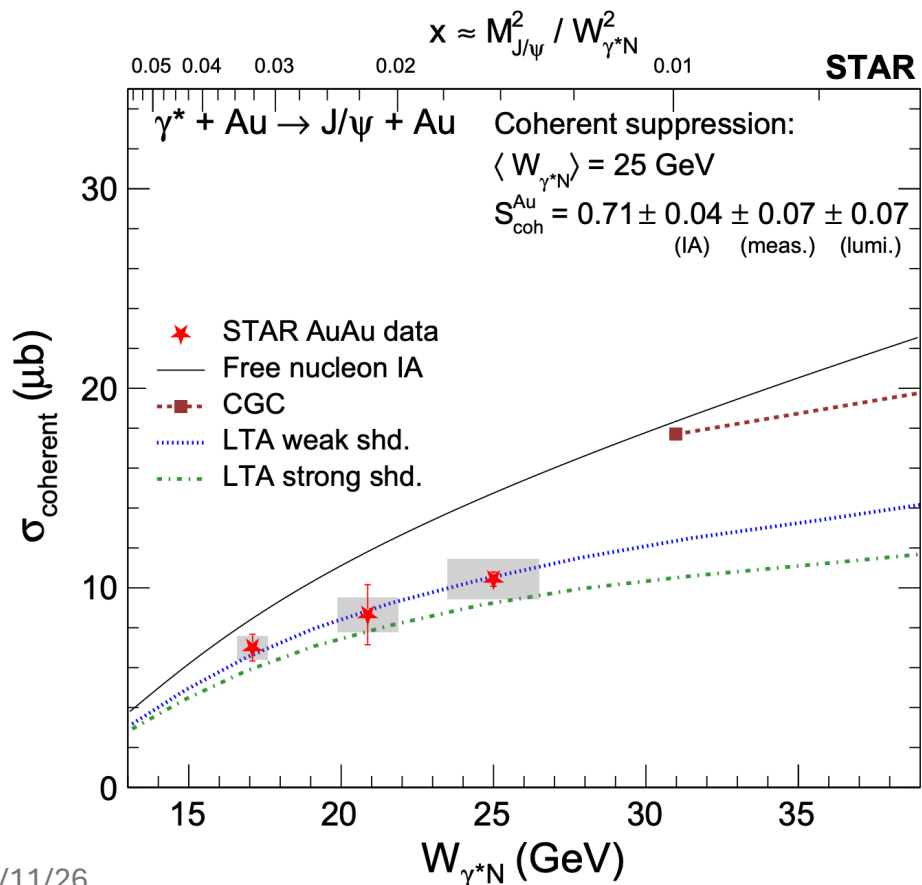
# Strong suppression of $J/\psi$ production in Au+Au UPCs

STAR, Phys. Rev. Lett. **133** (2024) 052301

STAR, Phys. Rev. C **110** (2024) 014911

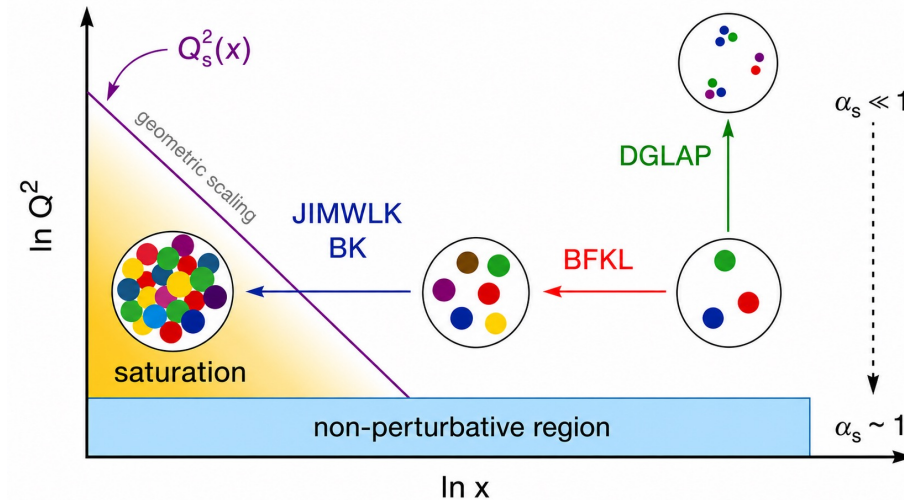
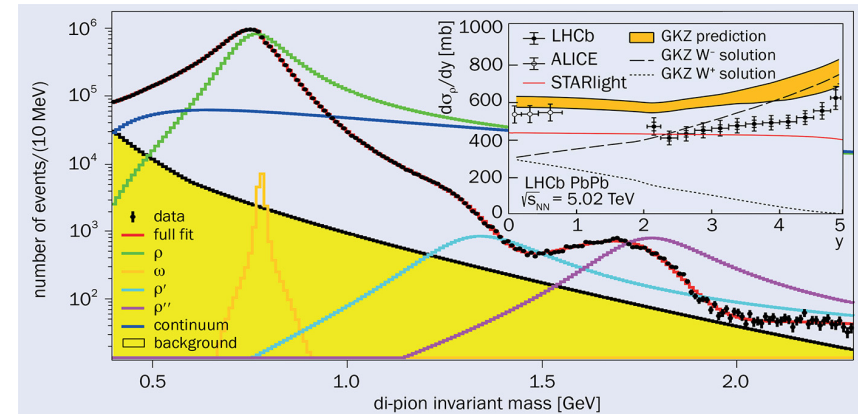
Coherent and incoherent  $J/\psi$  measurements.  
 $J/\psi$  coherent measurement with photon energy  
 $\psi(2S), e^+e^-$  production (not shown here)

Strong suppression for both coherent and incoherent  $J/\psi$   
 Coherent  $J/\psi$  suppression described well by weak  
 shadowing model.



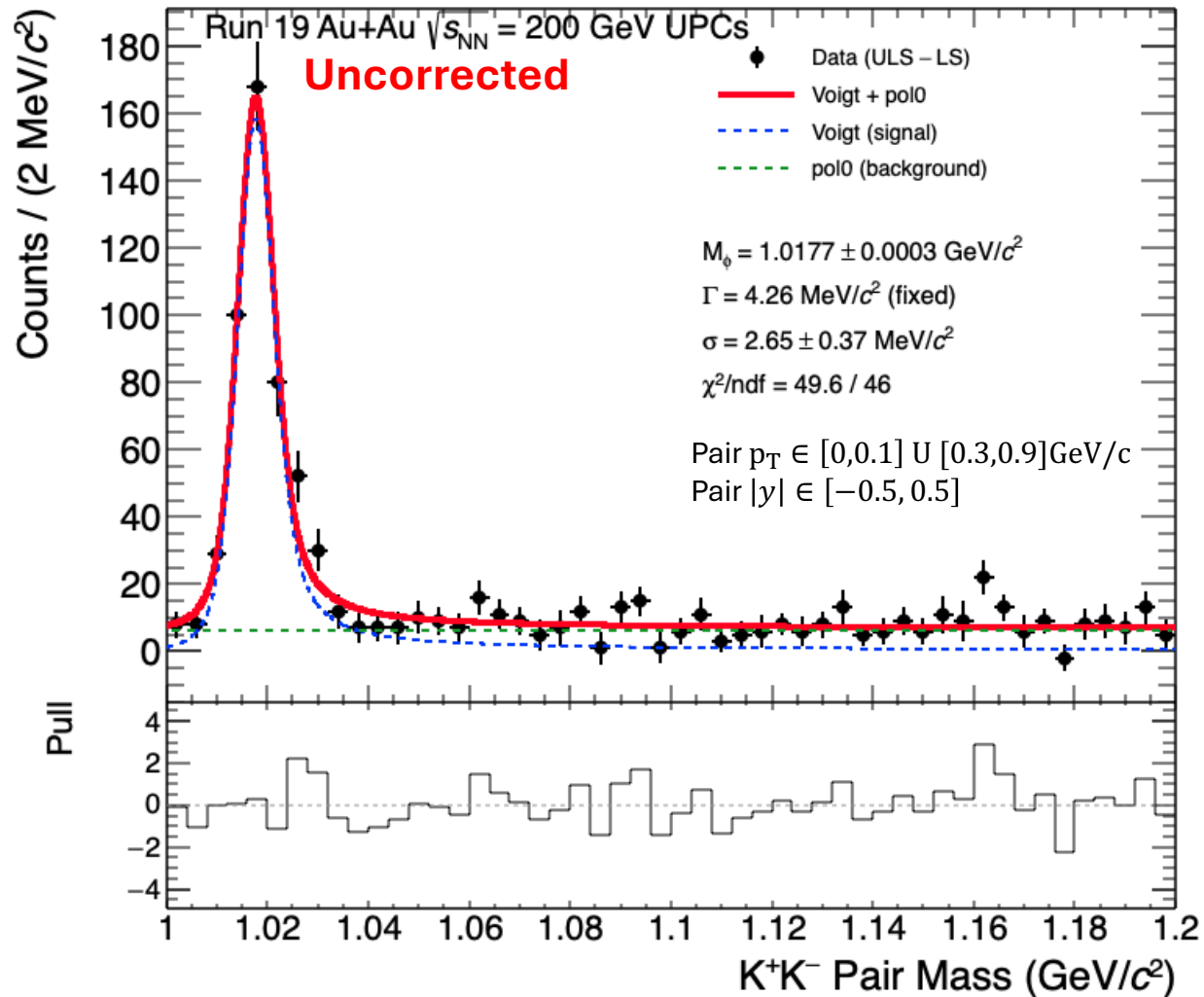
# What's Next?

- Full use of EESI to higher  $\pi^+\pi^-$  mass spectrum
- $\phi$  Measurement – transition region
  - More tomography via  $|t|$  fitting
- A-dependence cross section
  - $A^{2/3}$  vs  $A^{4/3}$  scaling
- $K^+K^-$  spectrum ...
- And so much more!



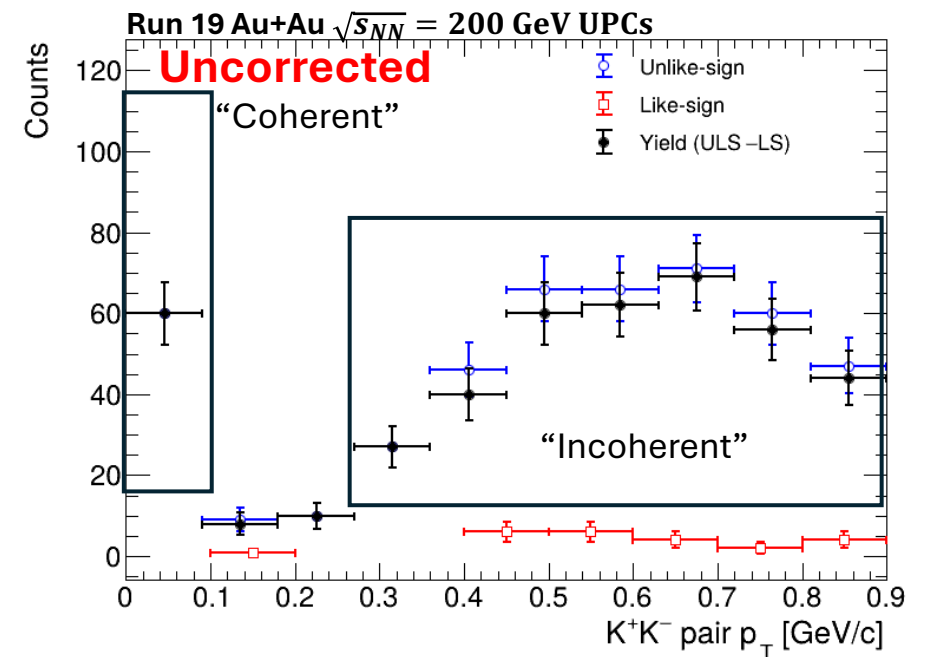
# A sneak peak – UPC $\phi$

Work in Progress



Run 19 Au+Au at  $\sqrt{s_{NN}} = 200$  GeV, **zdcmb**  
**First dataset with iTPC**

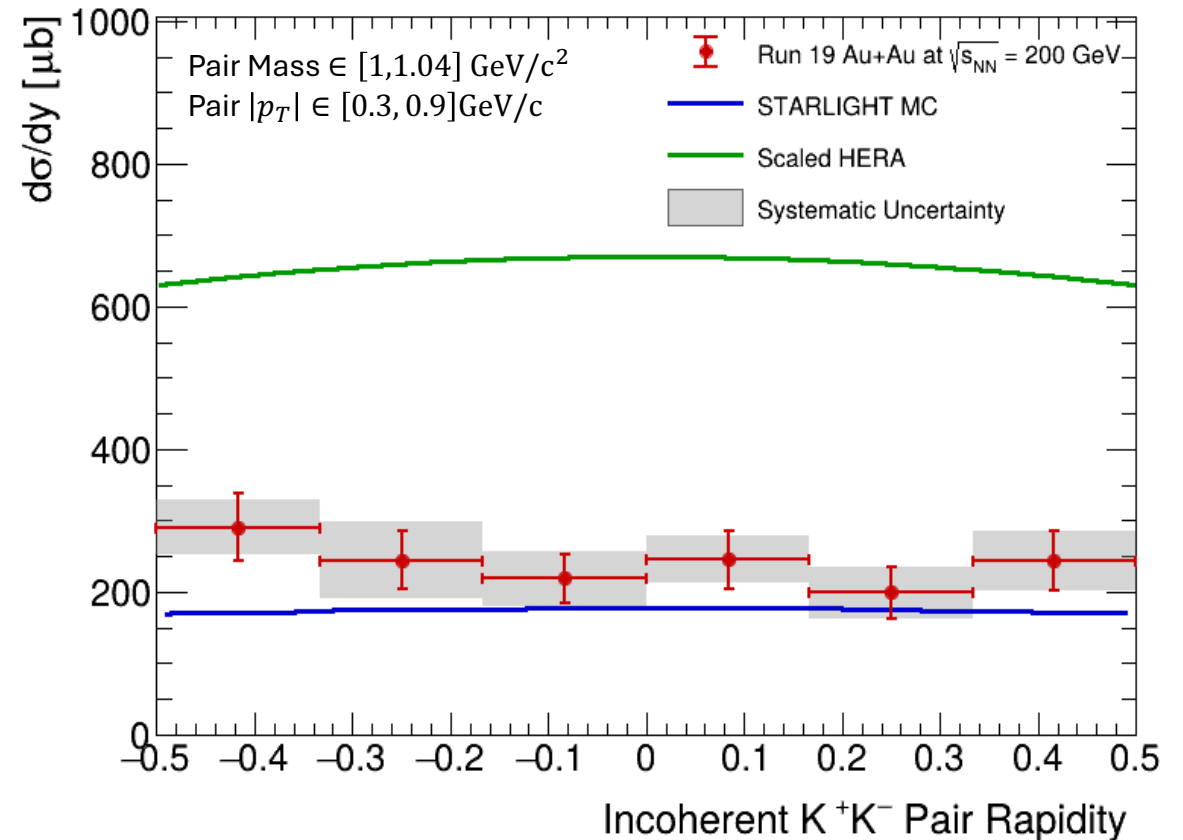
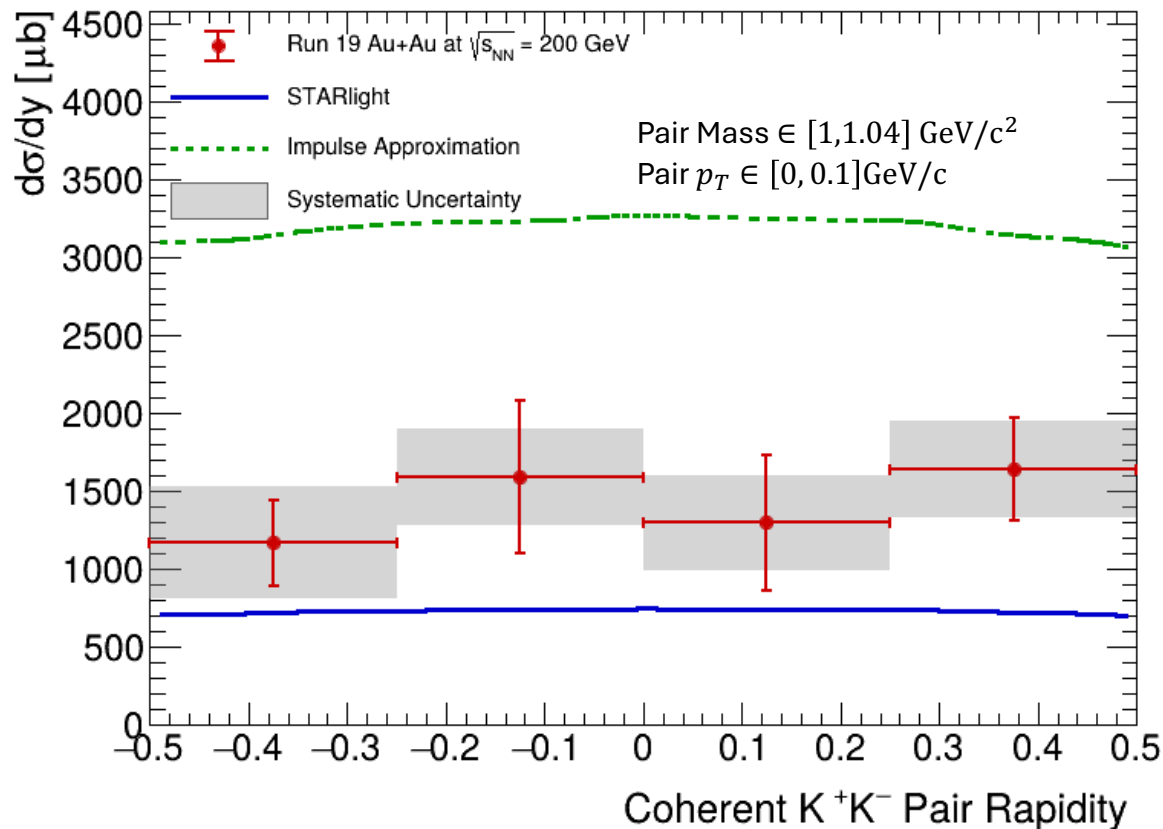
Signal region:  $M_{KK} \in [1, 1.04] \text{ GeV}/c^2$   
 # Coherent Pairs ( $p_T < 0.1 \text{ GeV}/c$ ): 61  
 # Incoherent Pairs: 358



# A sneak peak – UPC $\phi$

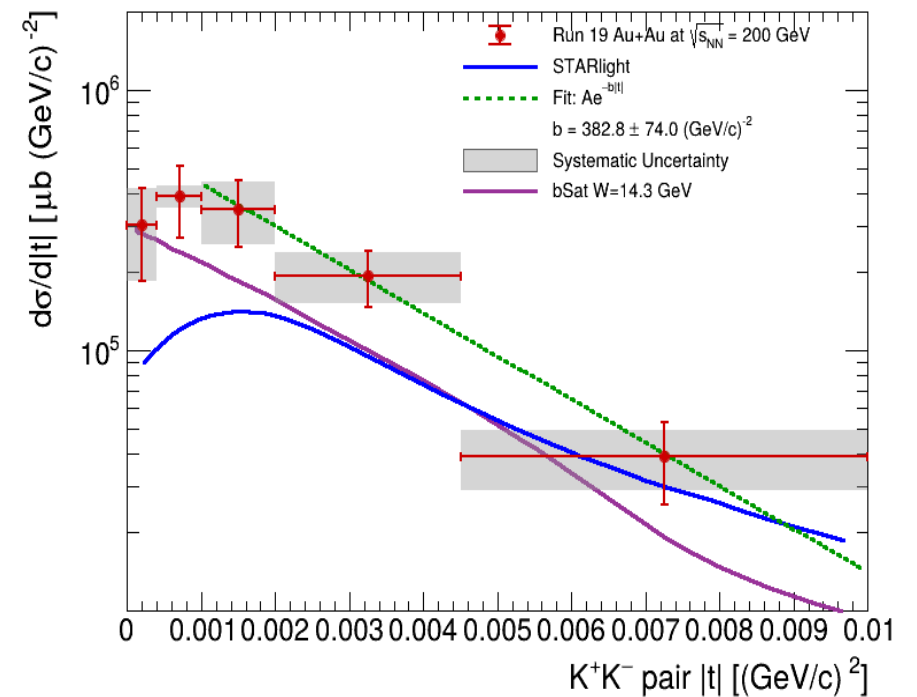
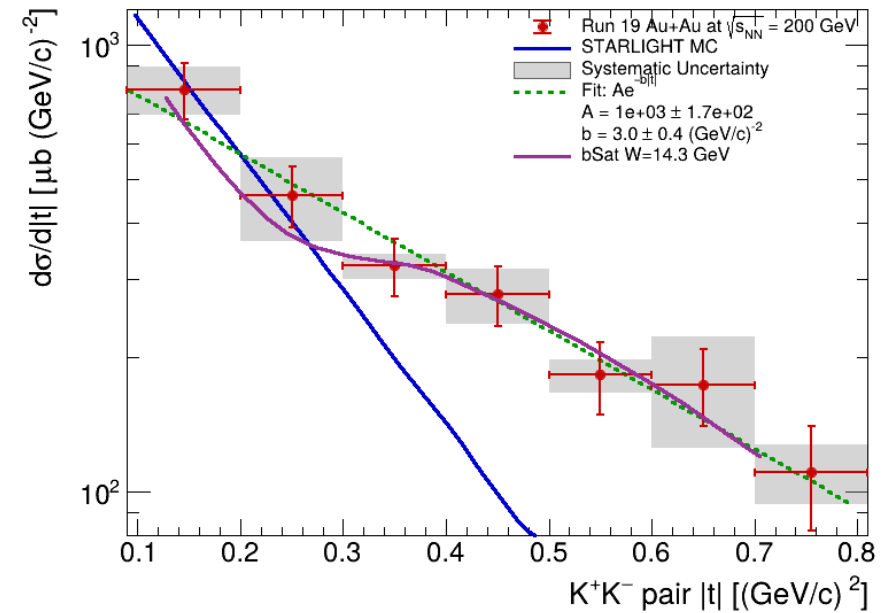
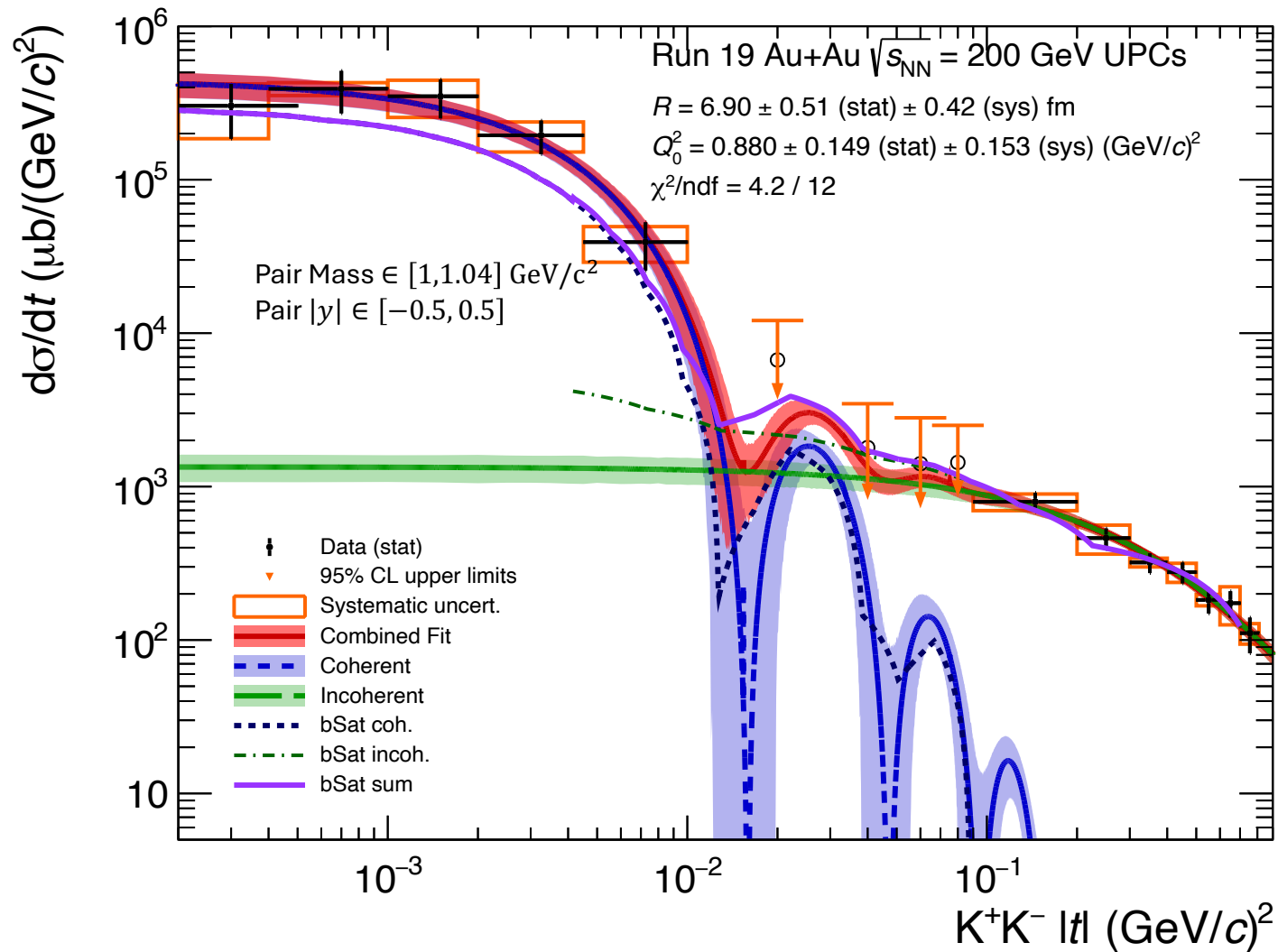
**STAR PRELIMINARY** 10% Luminosity, 7% Tracking Global Scale Uncertainty Not Shown

**Strong suppression compared with impulse approximation (coherent) and scaled HERA data (incoherent)**



# A sneak peak – UPC $\phi$

**STAR PRELIMINARY** 10% Luminosity, 7% Tracking Global Scale Uncertainty Not Shown



# Summary

- STAR established UPCs at RHIC as a clean photonuclear laboratory.
- STAR showed that UPCs are sensitive not only to nuclear size, but also to nuclear quantum interference.
- The light-vector-meson program evolved from cross sections to diffraction and nuclear imaging.
- STAR extended UPC physics from soft vector mesons to hard gluon probes.